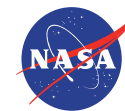




Spatial dependence of carrier localization in InAsSb/InSb digital alloy nBn detector

Brian Pepper, Alex Soibel, David Ting, Cory Hill, Arezou Khoshakhlagh,
Anita Fisher, Sam Keo, Sarath Gunapala

Center for Infrared Photodetectors, Jet Propulsion Laboratory, California
Institute of Technology, 4800 Oak Grove Dr., Pasadena, CA, 91109, USA



Jet Propulsion Laboratory
California Institute of Technology

Material robustness

Semiconductor families for infrared photodetection

	Si	Ge	GaAs	AlAs	InP	InGaAs	AlInAs	InAs	GaSb	AlSb	InSb	HgTe	CdTe
Group	IV	IV	III-V	III-V	III-V	III-V	III-V	III-V	III-V	III-V	III-V	II-VI	II-VI
Lattice Constant [Å]	5.431	5.658	5.653	5.661	5.870	5.870	5.870	6.058	6.096	6.136	6.479	6.453	6.476
Bulk Modulus [Gpa]	98	75	75	74	71	69	66	58	56	55	47	43	42
Direct Gap [eV] (λ [μm])	-	-	1.426 (0.87)	-	1.350 (0.92)	0.735 (1.69)	-	0.354 (3.5)	0.730 (1.7)	-	0.175 (7.1)	-0.141	1.475
MWIR/ LWIR Detection Mechanism	Heterojunction Internal photoemission (HIP)		Quantum well/dot Intersubband (QWIP/ QDIP)		Quantum well Intersubband (QWIP)			Bulk (MW) / Superlattice (MW/LW) Band-to-Band			Bulk B-B	Bulk Band-to-Band	

General Trends

Larger lattice constant

Weaker chemical bond (less covalent / more ionic)

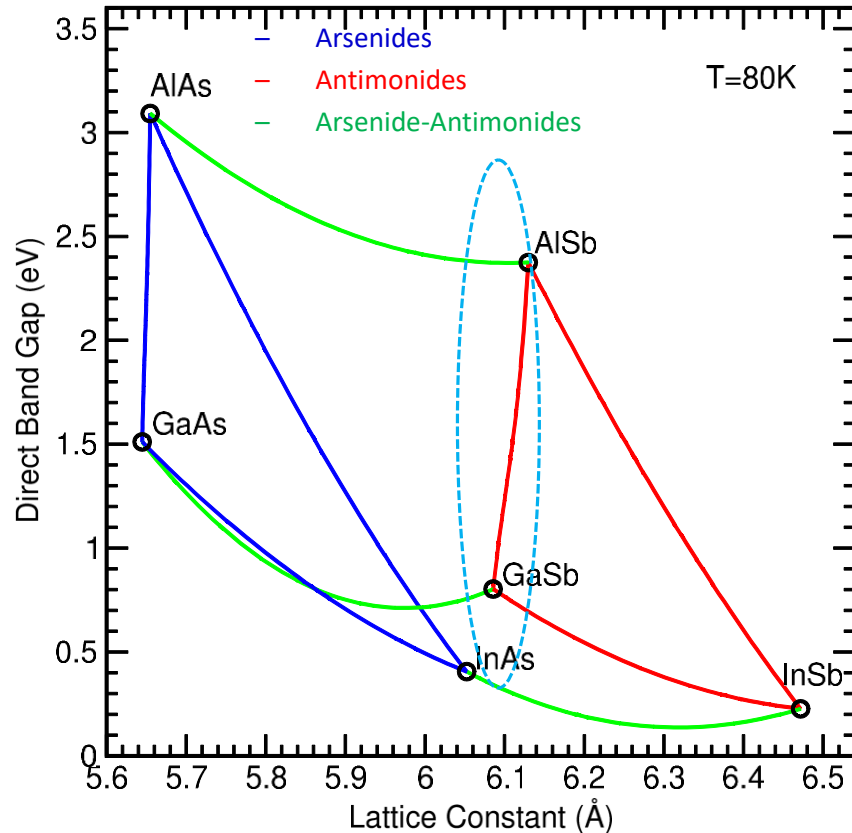
Decreasing material robustness / manufacturability

Smaller band gap (enables strong band-to-band IR absorption)

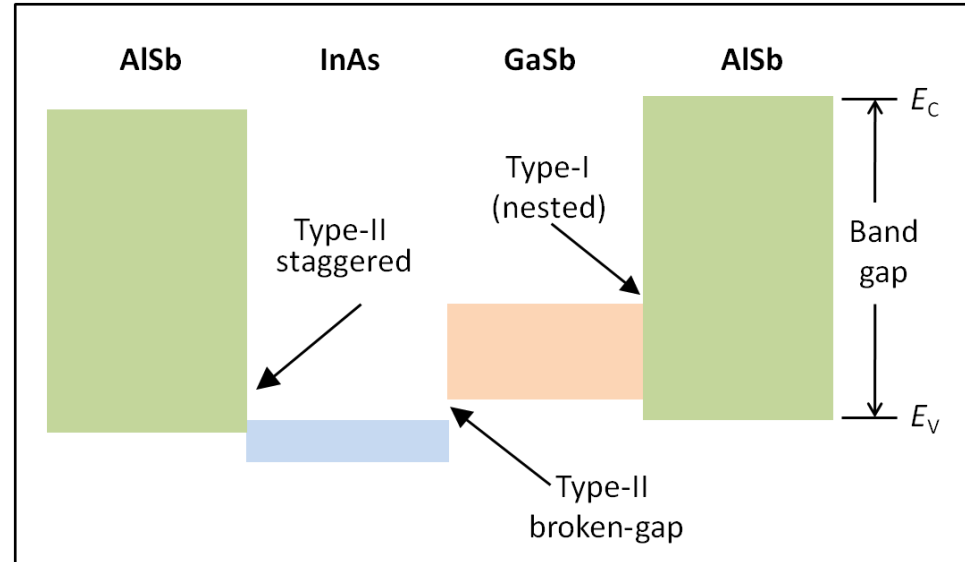
Higher quantum efficiency

Spatial dependence of carrier localization in InAsSb/InSb digital alloy
nBn detector

Antimonides for type-II superlattices

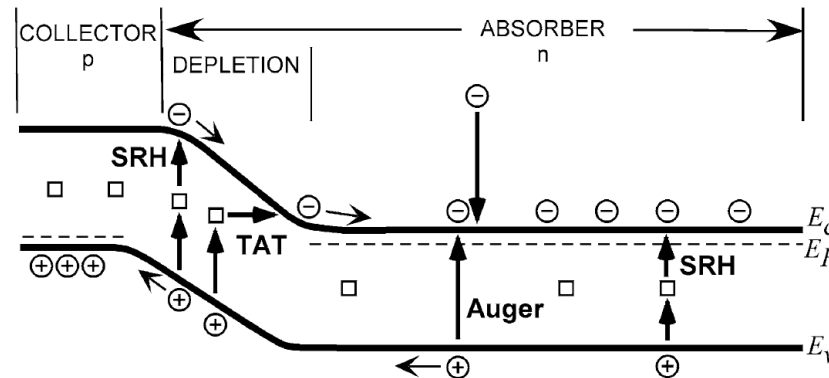


- Material system includes InAs, GaSb, AlSb and their alloys
 - Nearly lattice matched (~ 6.1 Å)
- Alloys with GaAs, AlAs, and InSb adds even more flexibility



- Three types of band alignments
 - Type-I (nested, straddling)
 - Type-II staggered
 - Type-II broken gap (misaligned, Type-III)
 - Unique among common semiconductor families
 - Overlap between InAs CB and GaSb VB enables interband devices
- Tremendous flexibility in artificially designed materials / device structures

Dark current mechanisms in a homojunction diode

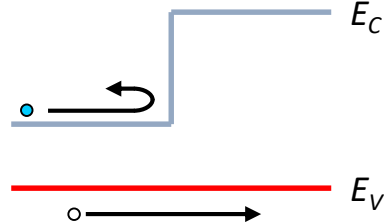


D. R. Rhiger, J. Electronic Materials, 40(8) 1815 (2011)

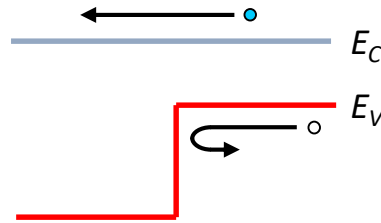
- High performance IR detector requires good signal (photoresponse; QE) to noise (dark current) ratio
 - High QE achieved using thick, strain-balanced absorbers
- Dark current mechanisms in a p-on-n homojunction
 - Trap assisted tunneling, band-to-band tunneling
 - G-R current from SRH processes in depletion region
 - Diffusion dark current from Auger and SRH processes in quasi-neutral region
 - Surface leakage current (not shown)
- Designs based on heterostructures can enhance performance

Unipolar barriers

Electron blocking barrier



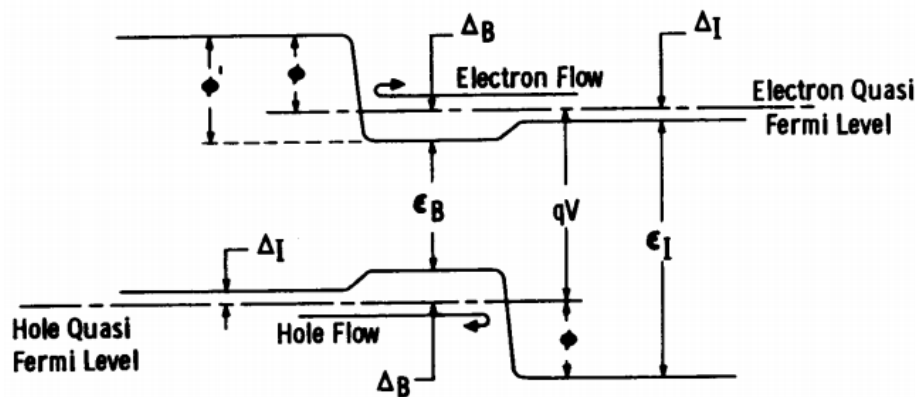
Hole blocking barrier



- Unipolar barriers:

- Block one carrier type, but allows unimpeded flow of the other
- Electron barrier
- Hole barrier
- Terminology introduced in Ting et al. *Appl. Phys. Lett.* **95**, 023508 (2009), now in common usage

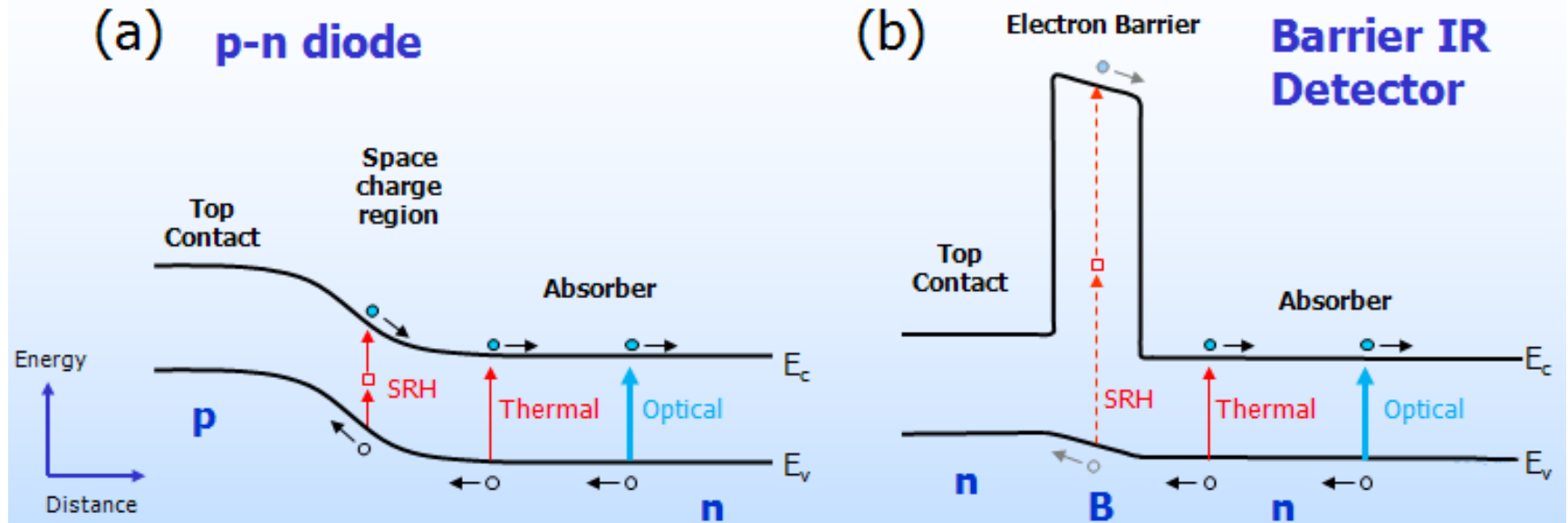
Double Heterostructure Laser



- Using unipolar barriers to enhance semiconductor device performance

- DH Laser, H. Kroemer, Proc. IEEE 1963
- DH Laser, Zh. I. Alferov and R. F. Kazarinov, patent certificate (Russian) 1963

nBn detectors



BIRD (nBn, XBn, pBn,..) utilizes unipolar barriers:

- Block one carrier type, but allows un-impeded flow of the other

BIRD advantages

- Suppressed generation-recombination current
- Simplified fabrication process utilizing shallow etching into the barrier
- Elimination of surface leakage currents

nBn utilizing an InAsSb/AlAsSb absorber-barrier combination

- The most successful implementation of BIRD
- Cut-off wavelengths in this design is limited to about $\lambda_c = 4 \text{ mm}$

Maimon, S., and G. W. Wicks (2006). nBn detector, an infrared detector with reduced dark current and higher operating temperature. Appl. Phys. Lett. 89, 151109

Klipstein, P. (2008). 'XBn' barrier photodetectors for high sensitivity and high operating temperature infrared sensors. Proc. SPIE 6940, 69402U-2.

June 20th, 2018

Spatial dependence of carrier localization in InAsSb/InSb digital alloy

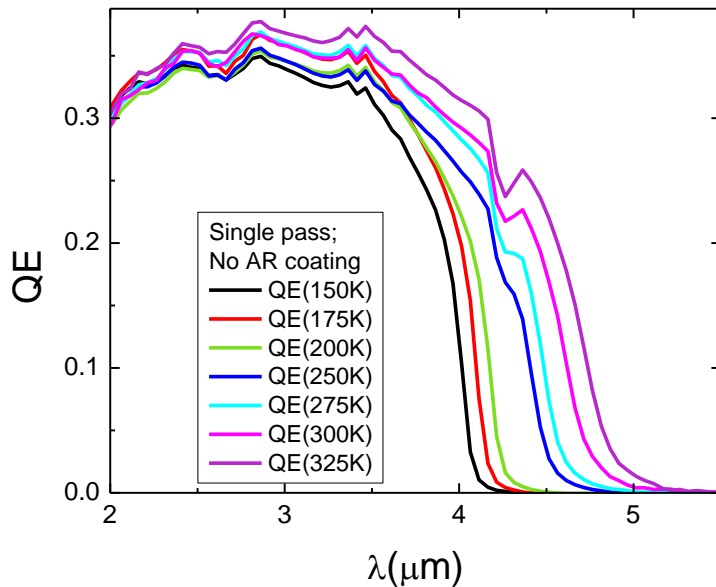
nBn detector

Pepper *et al.*

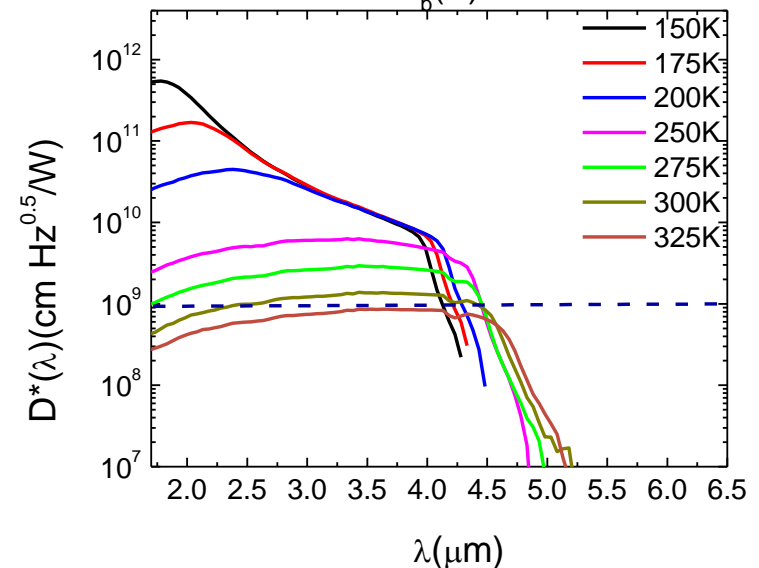
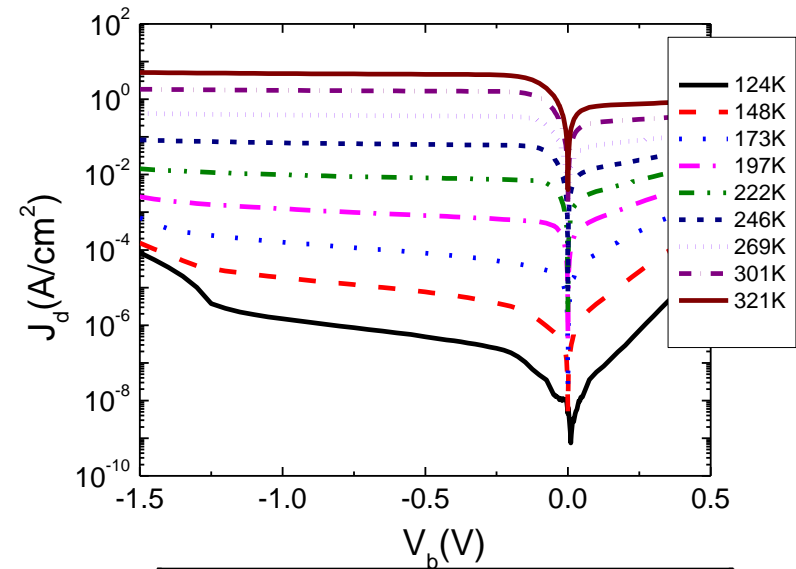


Jet Propulsion Laboratory
California Institute of Technology

Bulk InAsSb nBn performance at high T

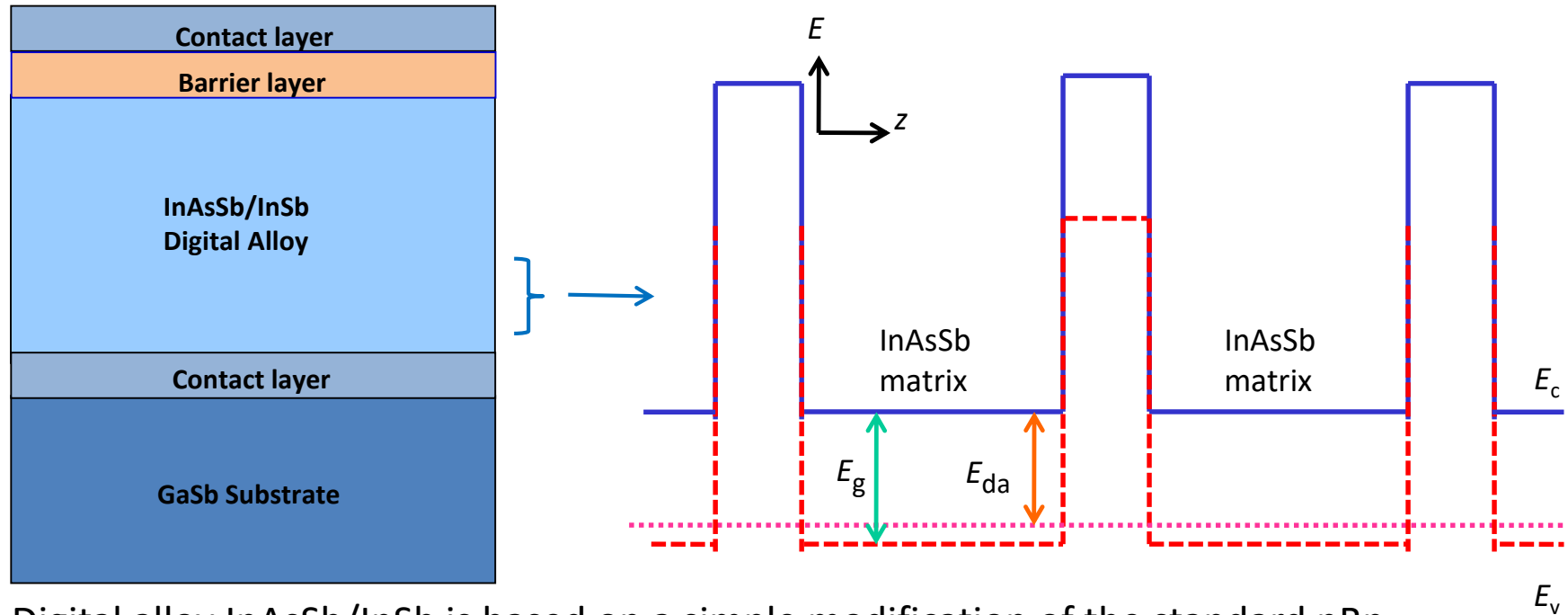


- Very good performance up to high temperatures
 - High QE
 - $\lambda_c = 3.8\mu\text{m}$ at $T = 77\text{K}$
 - $\lambda_c = 4.7\mu\text{m}$ at $T = 325\text{K}$
 - Low dark current
 - $j_d = 7 \times 10^{-7} \text{ A/cm}^2$ at $T = 148\text{K}$
 - $j_d = 6 \times 10^{-2} \text{ A/cm}^2$ at $T = 246\text{K}$
 - High Detectivity
 - BLIP below 225K
 - $D^*(\lambda) = 5 \times 10^9 \text{ (cm Hz}^{0.5}/\text{W)}$ at 250K



InAsSb/InSb digital alloy

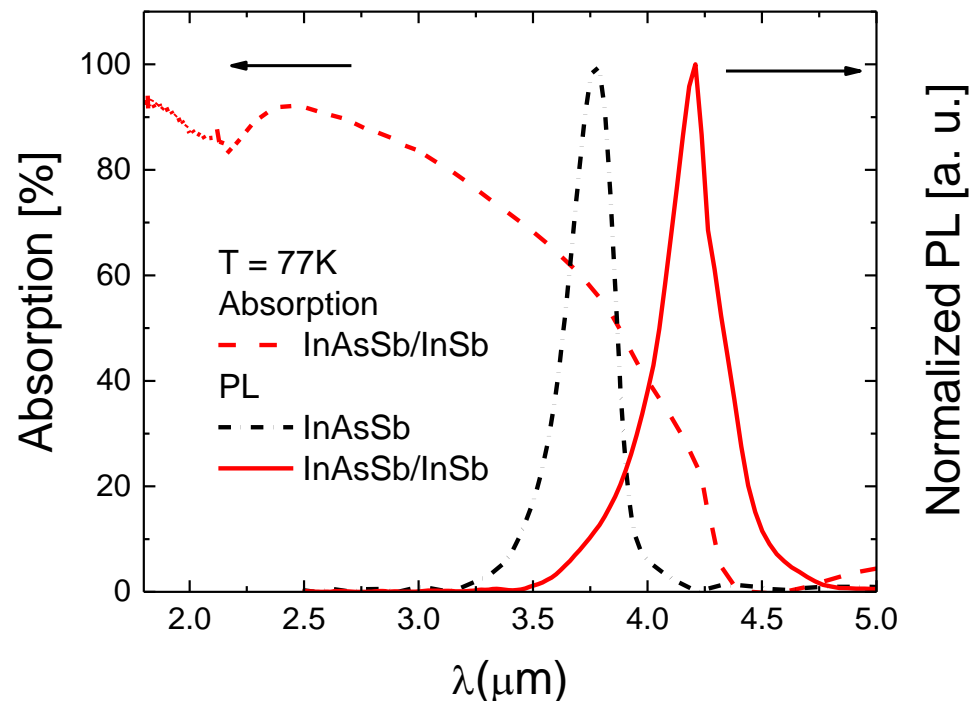
How to extend cut-off wavelength of InAsSb BIRD detectors?



- Digital alloy InAsSb/InSb is based on a simple modification of the standard nBn
- Periodic insertion of InSb monolayers
 - 1 InSb monolayer to 14 monolayers of $\text{InAs}_{0.92}\text{Sb}_{0.08}$ (period 4.5 nm)
- Type-II broken-gap band alignment between InSb and InAsSb
- New level in valence band of InSb monolayer
 - Transition energy $E_{da} < E_g$, where E_g is InAsSb bandgap

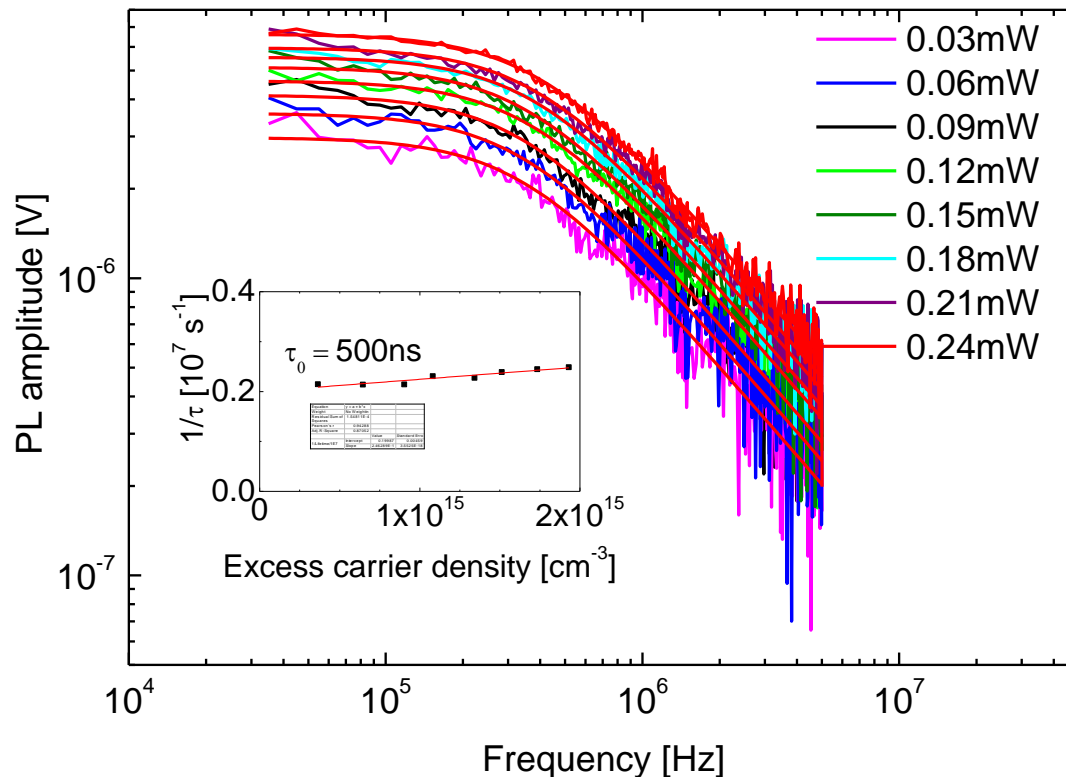
A. Soibel *et al.*, Mid-wavelength infrared InAsSb/InSb nBn detector with extended cut-off wavelength, Applied Physics Letters 109, 103505 (2016)

PL and absorption



- At $T = 77\text{K}$, the digital alloy exhibits PL peak = $4.21\mu\text{m}$
 - Compared to the = $3.79\mu\text{m}$ of $\text{InAs}_{0.915}\text{Sb}_{0.085}$ bulk material
 - Compared to the = $5.5\mu\text{m}$ of InSb QD embedded in $\text{InAs}_{0.915}\text{Sb}_{0.085}$ bulk material
- The absorption spectrum of the $2\mu\text{m}$ thick digital alloy absorber is shown above
 - Absorption is $a = 70\%$ and the absorption coefficient is $a_c = 2900\text{ cm}^{-1}$ at $\lambda = 3.4\mu\text{m}$
- The transmission of the GaSb substrate used for the growth of these devices was found to be higher than $>95\%$ for $\lambda < 6\mu\text{m}$

Minority carrier lifetime



- The minority carrier lifetime in the digital alloy, $\tau_{da} = 500 \text{ ns}$, at $T = 77 \text{ K}$
- The estimated radiative recombination time $\tau_r = 470\text{-}570 \text{ ns}$
 - From the absorption spectrum and the carrier concentration, $n_{\text{abs}} = 3\text{-}4 \times 10^{14} \text{ cm}^{-3}$
 - Close to the experimentally measured lifetime
 - Radiative recombination controls the minority carrier lifetime at $T = 77 \text{ K}$
- The minority carrier lifetime in $\text{InAs}_{0.915}\text{Sb}_{0.085}$ bulk material $\tau_{\text{bulk}} = 300 \text{ ns}$
 - For carrier concentration of $n = 1\text{-}2 \times 10^{15} \text{ cm}^{-3}$

Carrier localization in InAsSb/InSb T2SLs

APPLIED PHYSICS LETTERS **107**, 201107 (2015)



Influence of carrier localization on minority carrier lifetime in InAs/InAsSb type-II superlattices

Zhi-Yuan Lin, Shi Liu, Elizabeth H. Steenberg^{a)} and Yong-Hang Zhang^{b)}

Center for Photonics Innovation and School of Electrical, Computer, and Energy Engineering, Arizona State University, Tempe, Arizona 85287, USA

(Received 18 October 2015; accepted 6 November 2015; published online 17 November 2015)

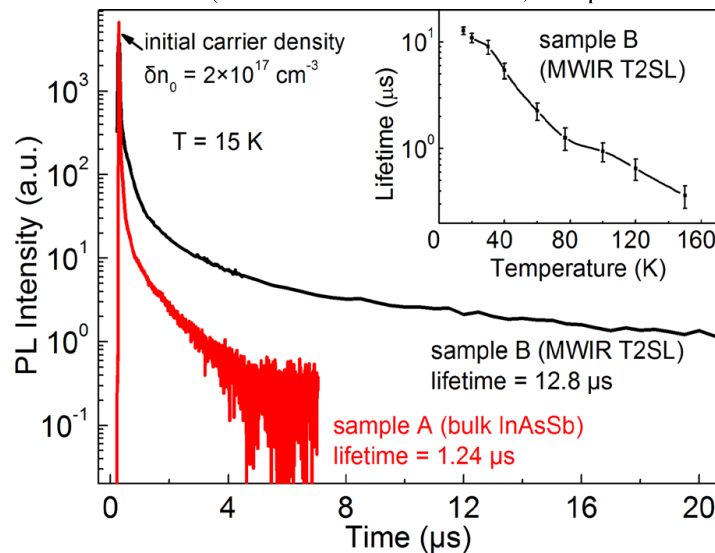


FIG. 1. Time-resolved photoluminescence decays of samples A (bulk InAsSb) and B (mid-wavelength infrared InAs/InAsSb type-II superlattice) at 15 K. The minority carrier lifetimes of 1.24 μs and 12.8 μs are extracted from the single exponential decays, respectively. The inset shows the carrier lifetime of sample B as a function of temperature.

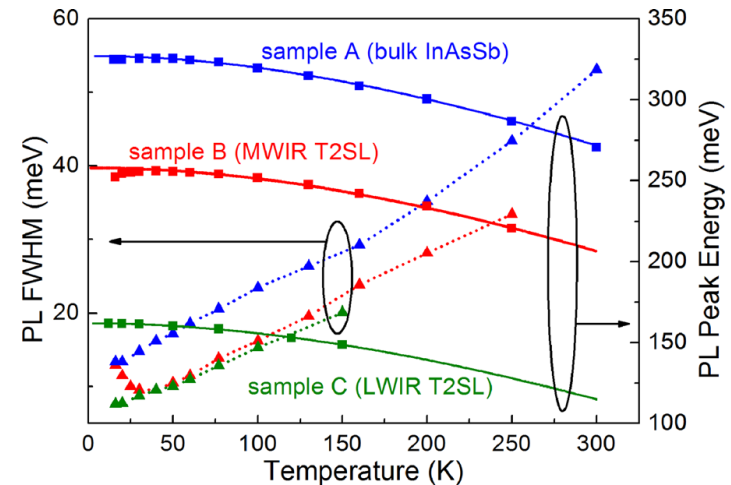


FIG. 2. Photoluminescence (PL) peak energy and full-width at half maximum (FWHM) of samples A (bulk InAsSb), B (MWIR InAs/InAsSb T2SL), and C (LWIR InAs/InAsSb T2SL) as a function of temperature. As temperature increases from 15 K to 50 K, the peak energy of sample B increases by 3 meV and the FWHM decreases by 3 meV, indicating carrier localization. The solid lines show the Varshni fit of PL peak energy as a function of temperature.

Carrier localization in InAsSb/InSb T2SLs (*cont.*)

APPLIED PHYSICS LETTERS **107**, 201107 (2015)



Influence of carrier localization on minority carrier lifetime in InAs/InAsSb type-II superlattices

Zhi-Yuan Lin, Shi Liu, Elizabeth H. Steenbergen,^{a)} and Yong-Hang Zhang^{b)}

Center for Photonics Innovation and School of Electrical, Computer, and Energy Engineering, Arizona State University, Tempe, Arizona 85287, USA

(Received 18 October 2015; accepted 6 November 2015; published online 17 November 2015)

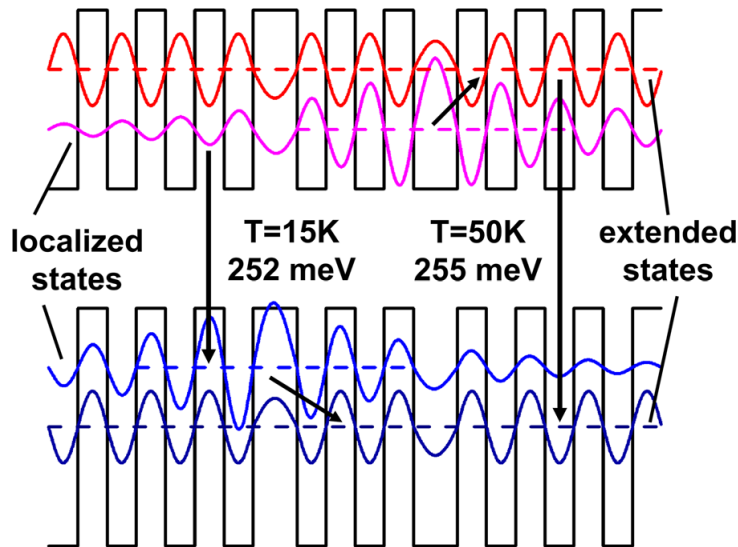


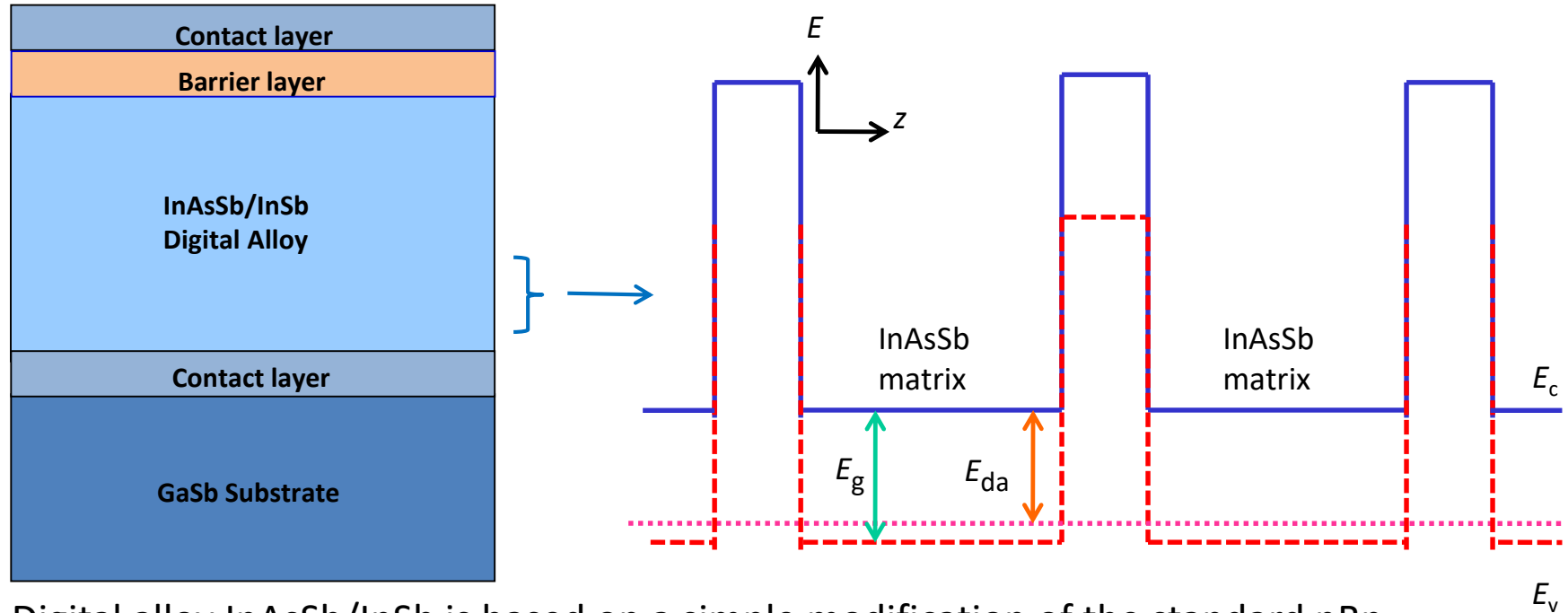
FIG. 3. Schematic representation of the carrier localization due to layer-to-layer thickness fluctuation. The localized states are generated when one layer is thicker than the surrounding layers in the superlattice. At low temperatures, the dominant optical transition occurs between the localized states. At temperatures greater than 50 K, the dominant optical transition occurs between extended states due to thermal de-localization.

- Hypothesis: localization caused by monolayer fluctuations.
- Localized states dominate at low T
- If true, SLs with shorter periods (than 9.9nm) should show increased effect

IDEA: Let's take this to the extreme

InAsSb/InSb digital alloy

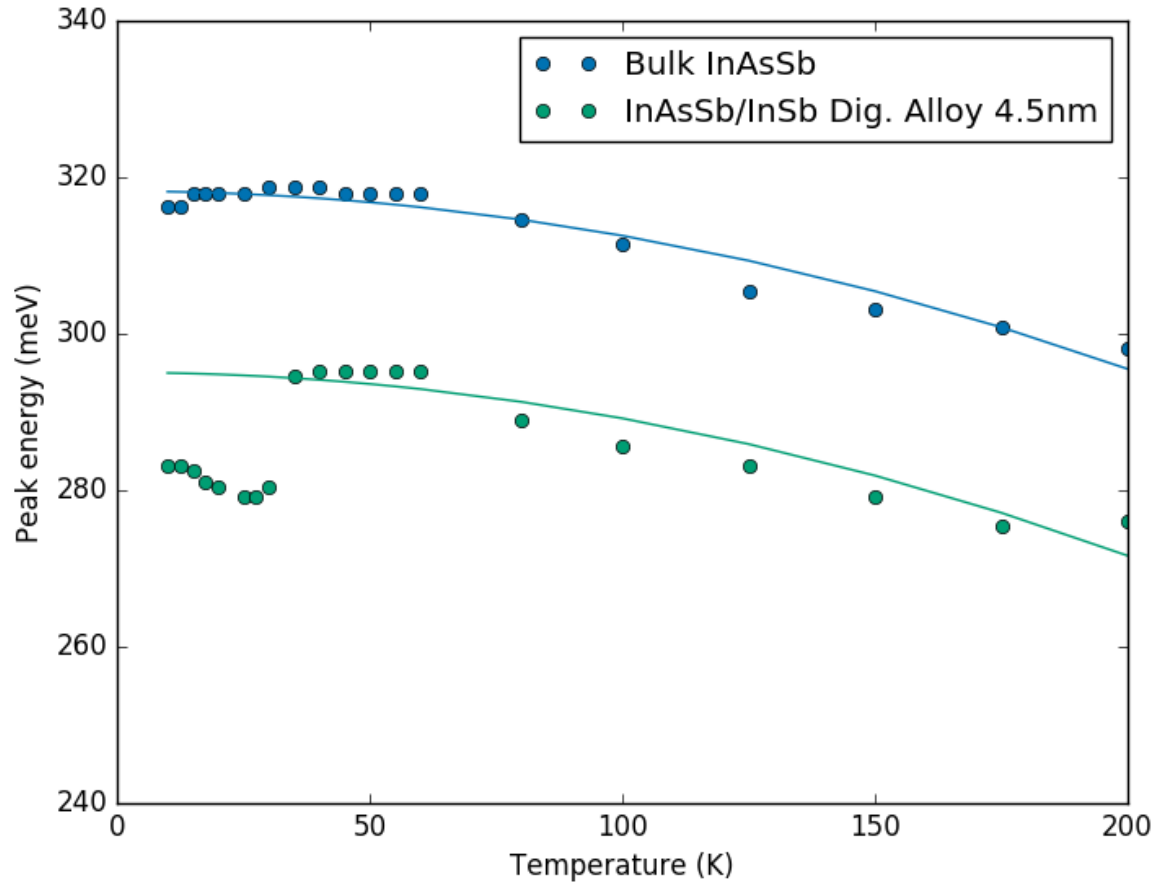
How to extend cut-off wavelength of InAsSb BIRD detectors?



- Digital alloy InAsSb/InSb is based on a simple modification of the standard nBn
- Periodic insertion of InSb monolayers
 - **1 InSb monolayer to 14 monolayers of InAs_{0.92}Sb_{0.08} (period 4.5 nm)**
- Type-II broken-gap band alignment between InSb and InAsSb
- New level in valence band of InSb monolayer
 - Transition energy $E_{da} < E_g$, where E_g is InAsSb bandgap

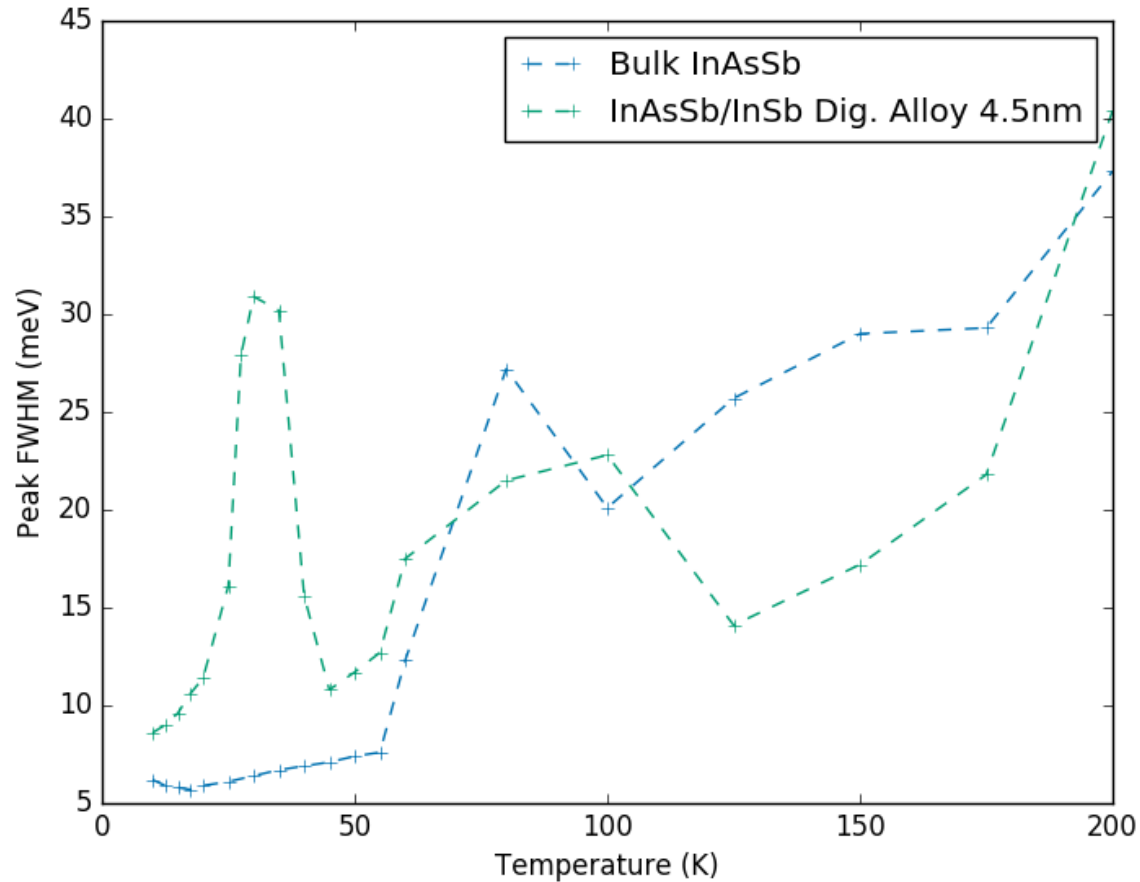
A. Soibel *et al.*, Mid-wavelength infrared InAsSb/InSb nBn detector with extended cut-off wavelength, Applied Physics Letters 109, 103505 (2016)

Bulk vs. digital alloy (PL peak)



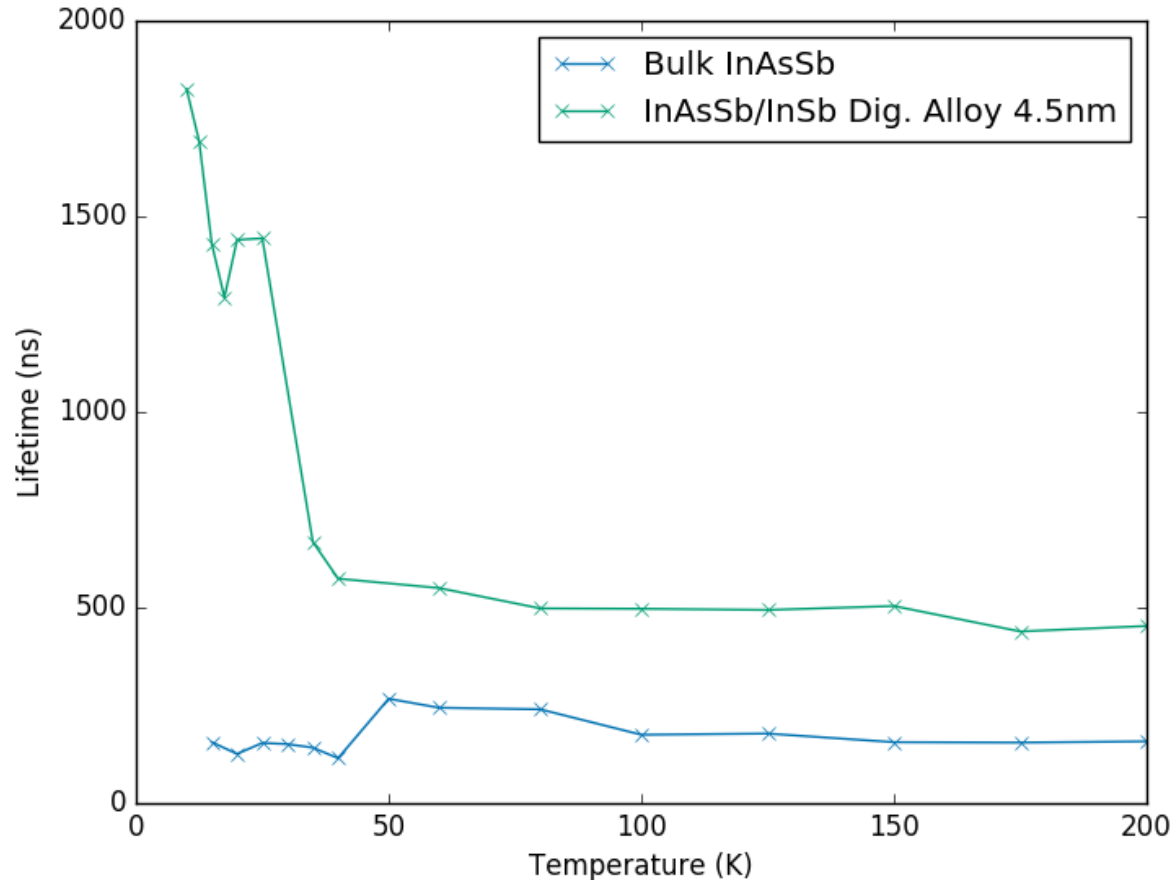
Digital alloy displays sudden 14 meV blue shift at 35 K

Bulk vs. digital alloy (FWHM)



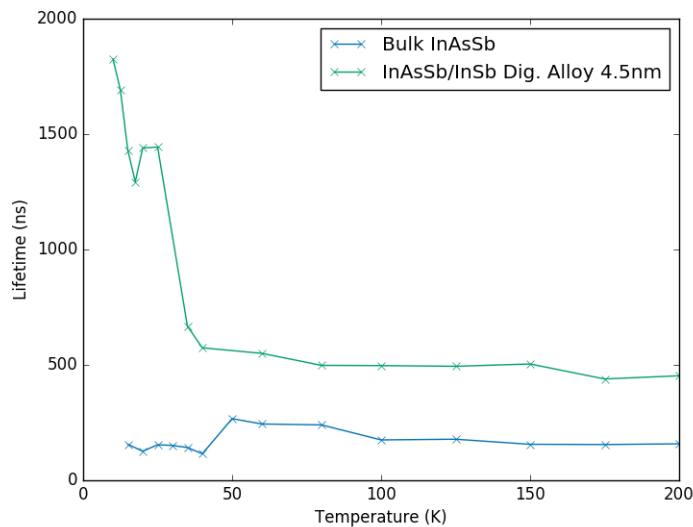
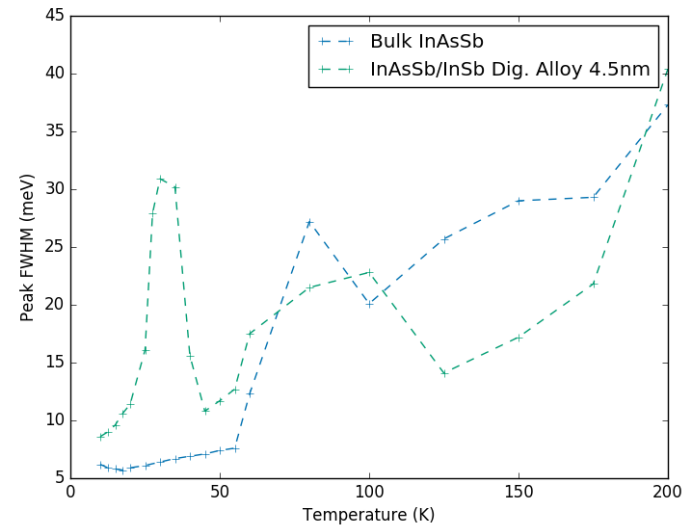
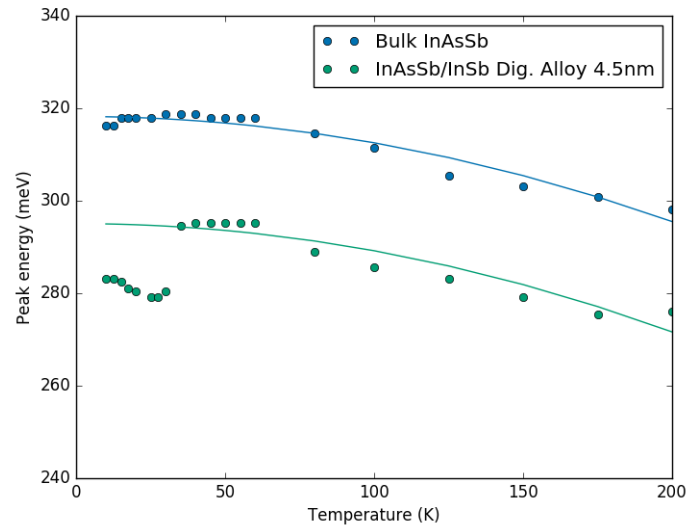
Digital alloy displays spike in FWHM as temperature falls below 35 K

Bulk vs. digital alloy (minority carrier lifetime)

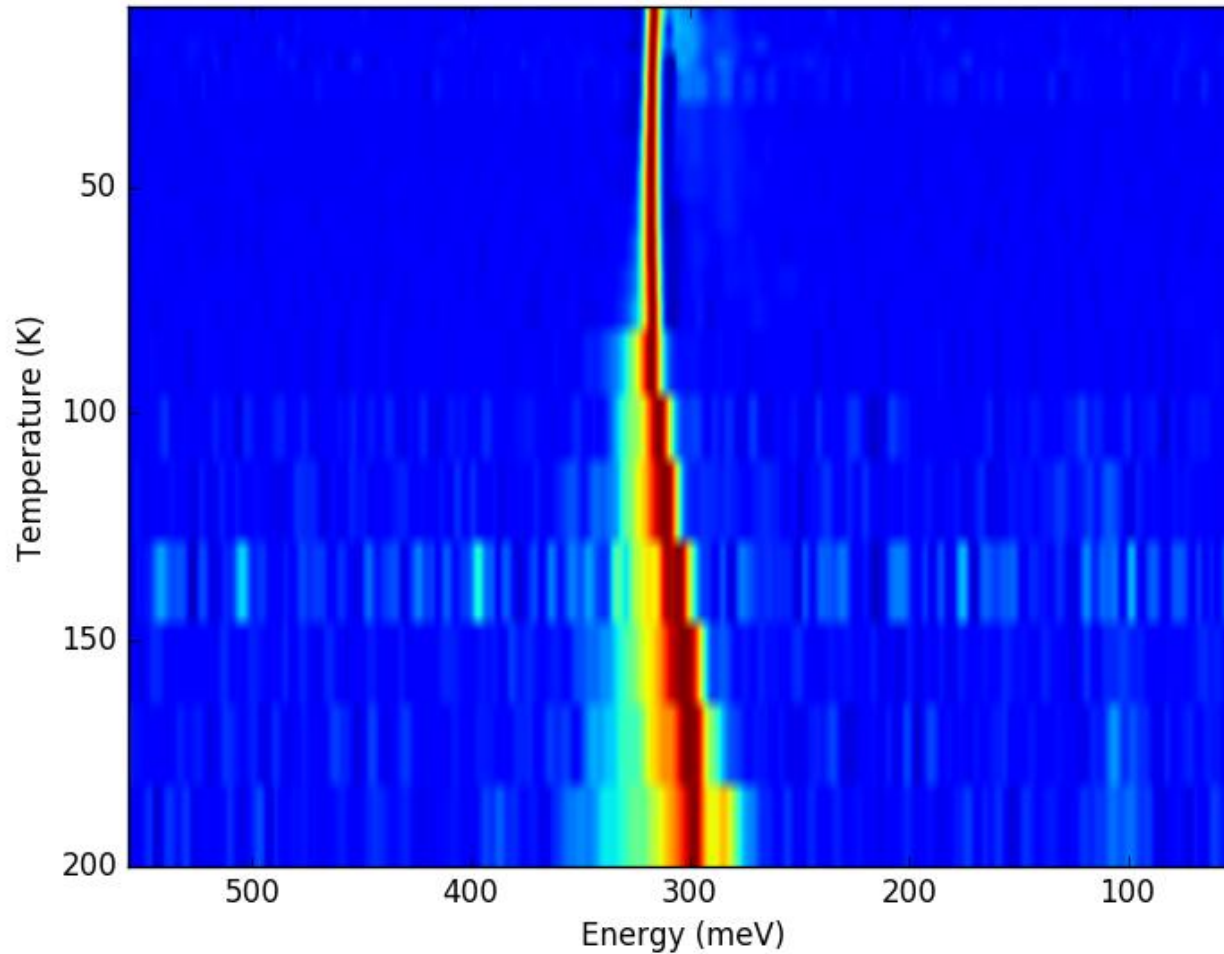


- Digital alloy displays spike in lifetime as temperature falls below 35 K
- Minority carrier lifetime measured by optical modulation response
- Donetsky et al., *APL* **97**, 052108 (2010)

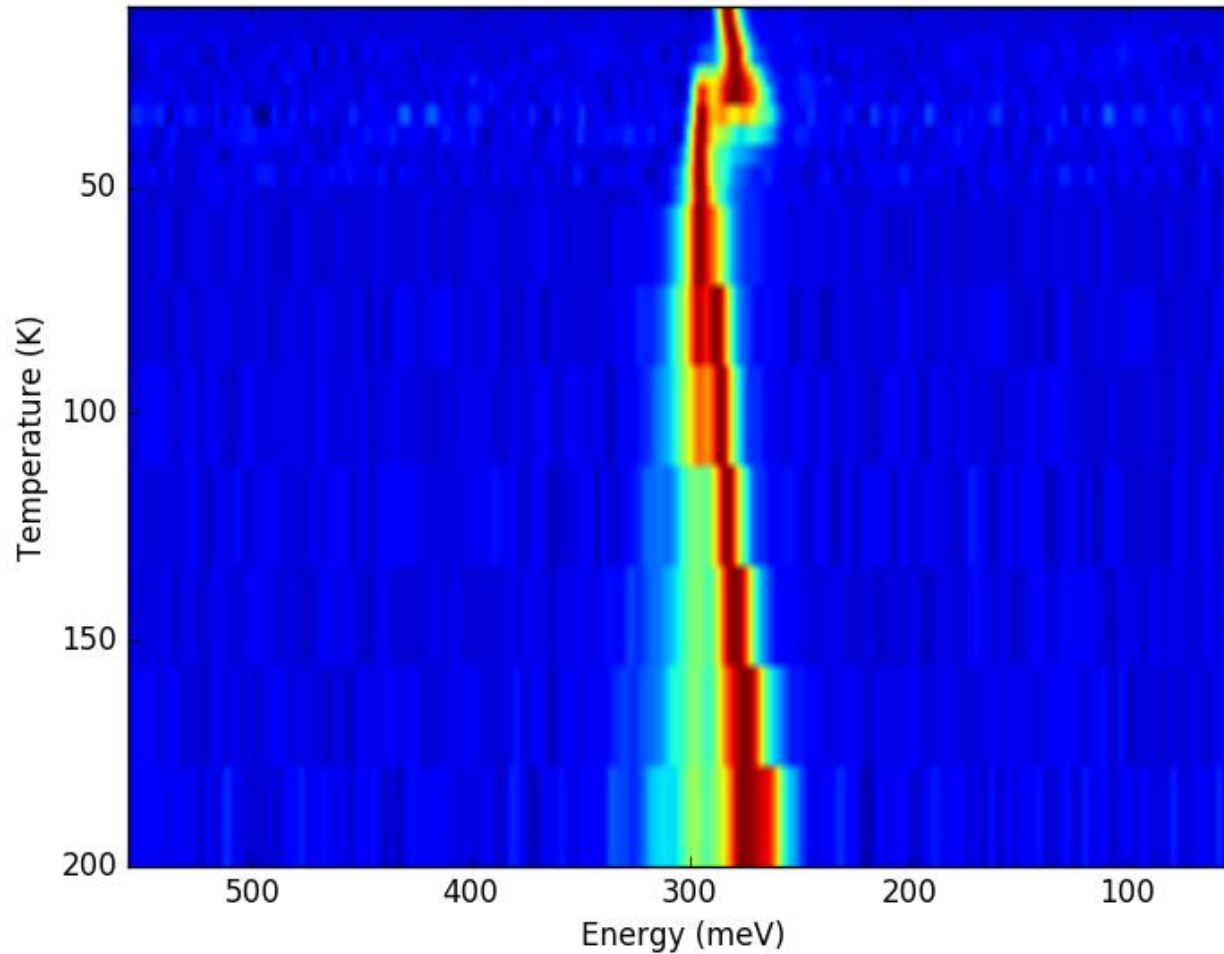
Comparison (bulk vs. digital alloy)



InAsSb Bulk



InAsSb/InSb digital alloy

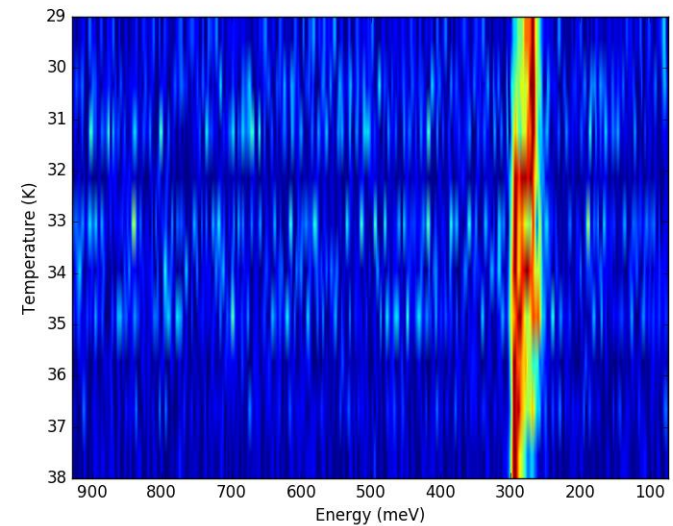
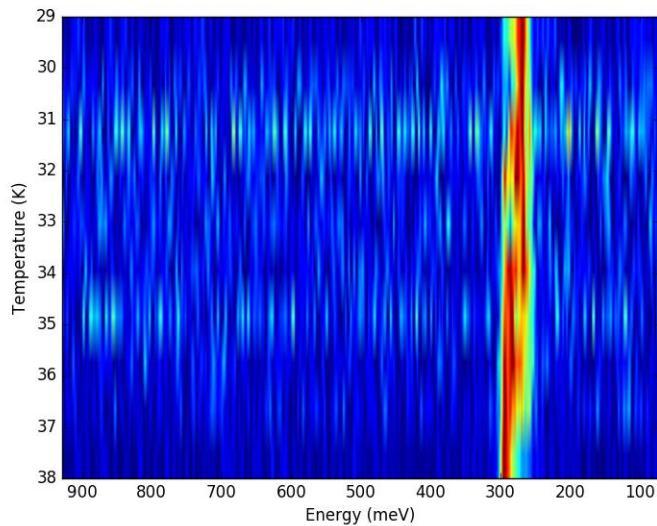
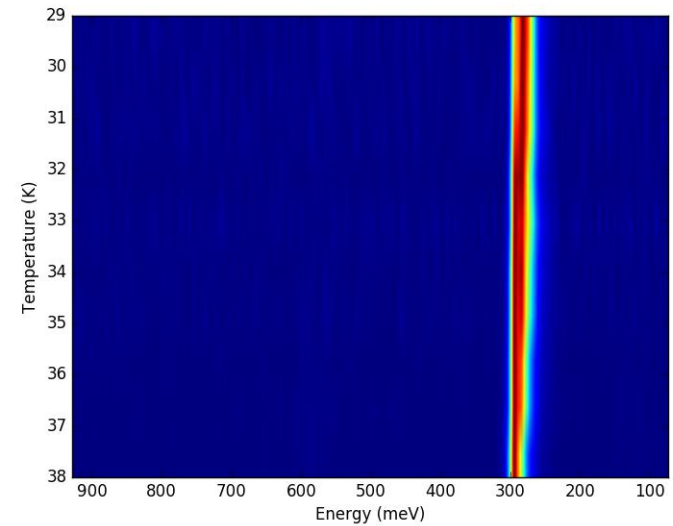
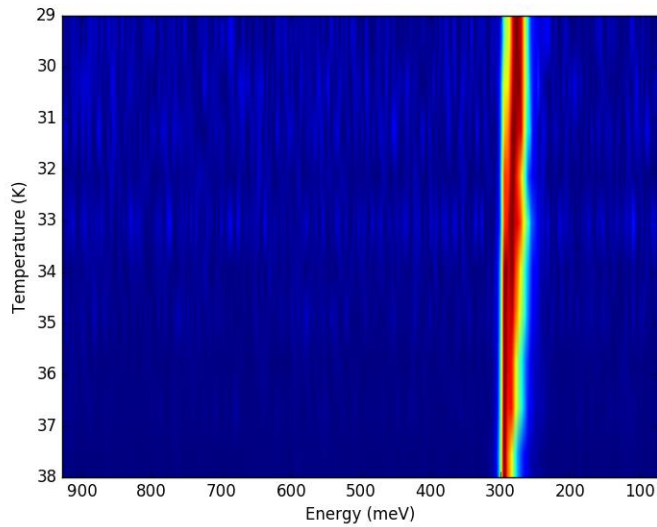


Spatial fluctuations?

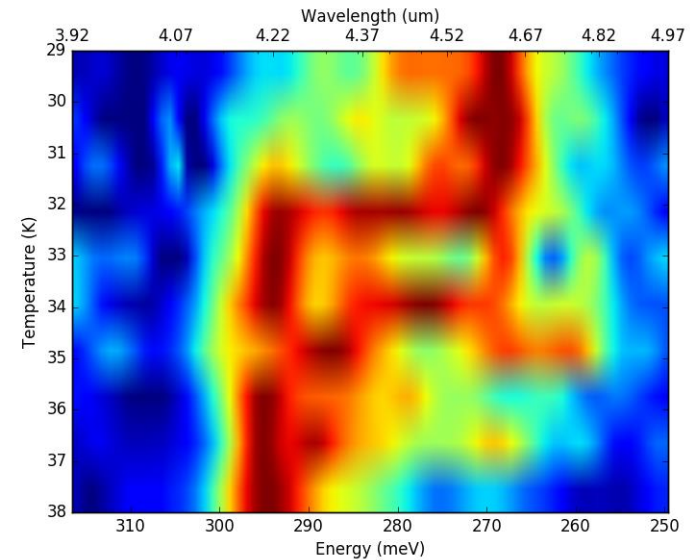
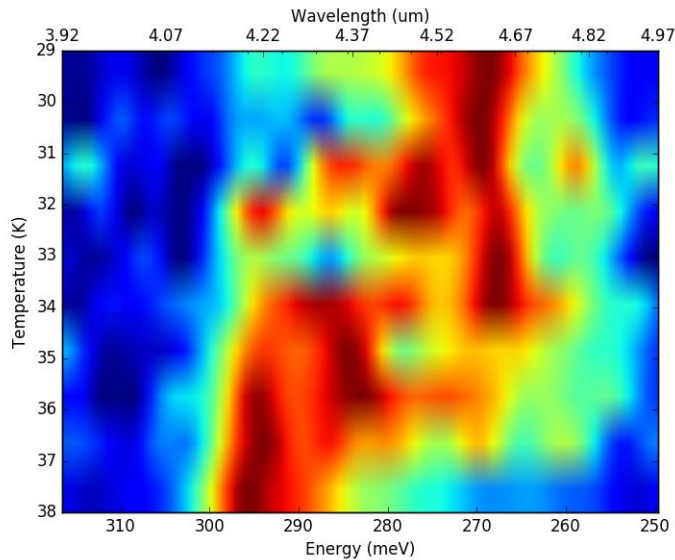
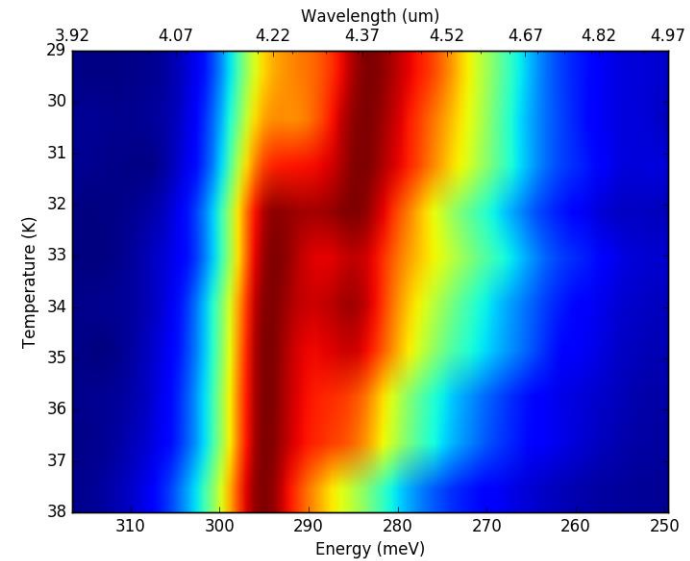
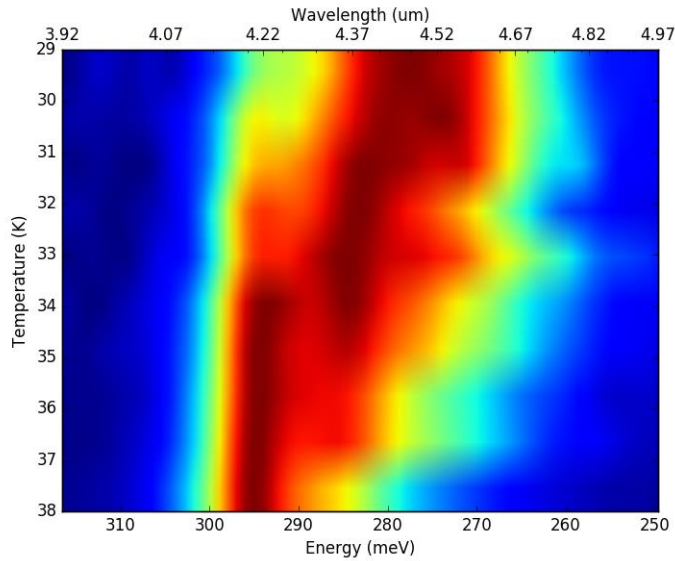
So how can we pin down whether these fluctuations are truly taking place?

- Idea: zoom in on the transition, taking spectra at 1 K steps, from 29-38 K.
- Measure at different spatial positions, using a 10x10 grid 3.81 mm x 3.81 mm wide
- Overall, 1000 spectra, time-consuming even when automated
- Look for spatial differences in the effect
- BUT: watch out for temperature gradient/edge effects!
 - Evidence effect was due to poor thermal contact and spatial differences in temperature

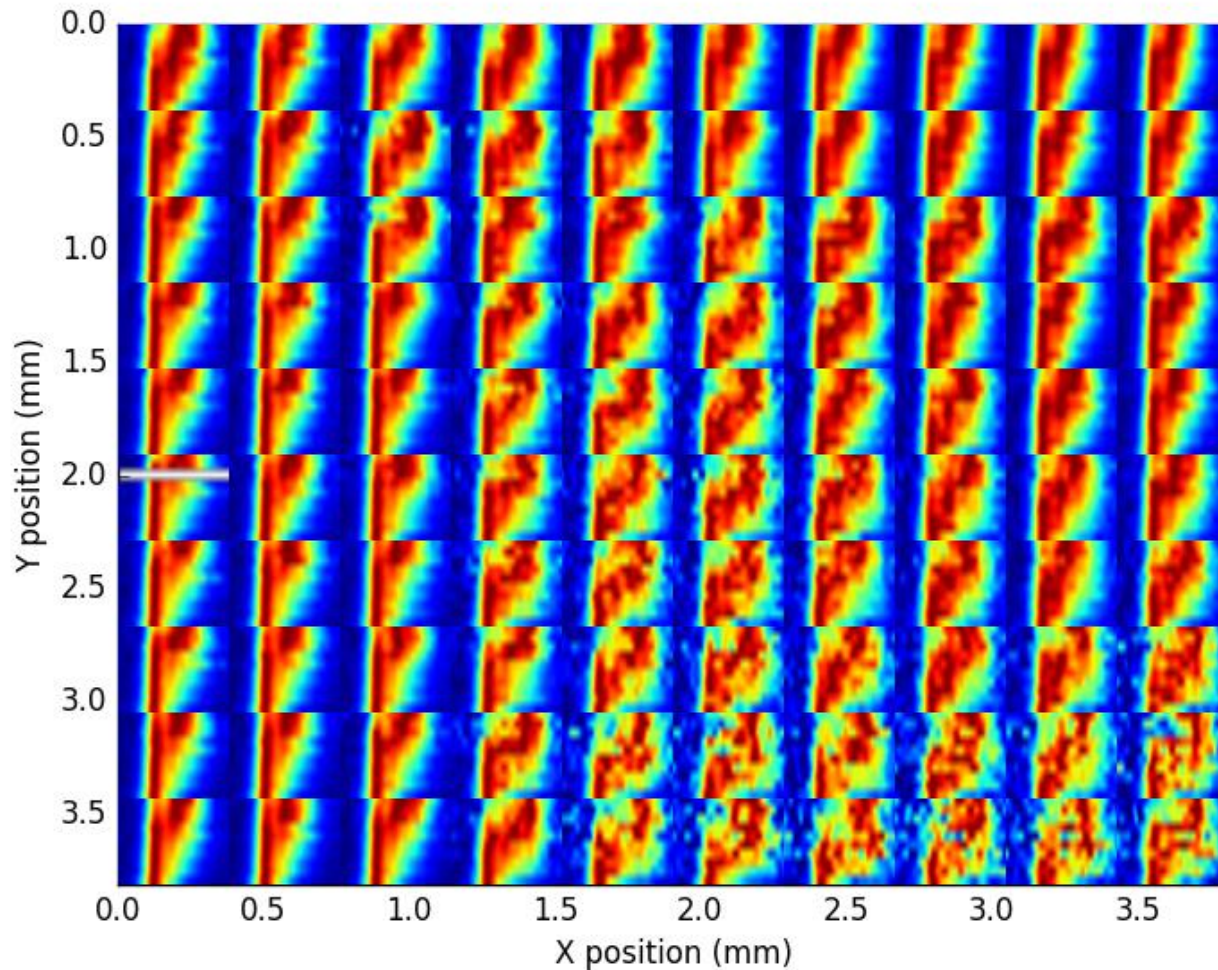
Example Spectra



Example Spectra (zoomed)



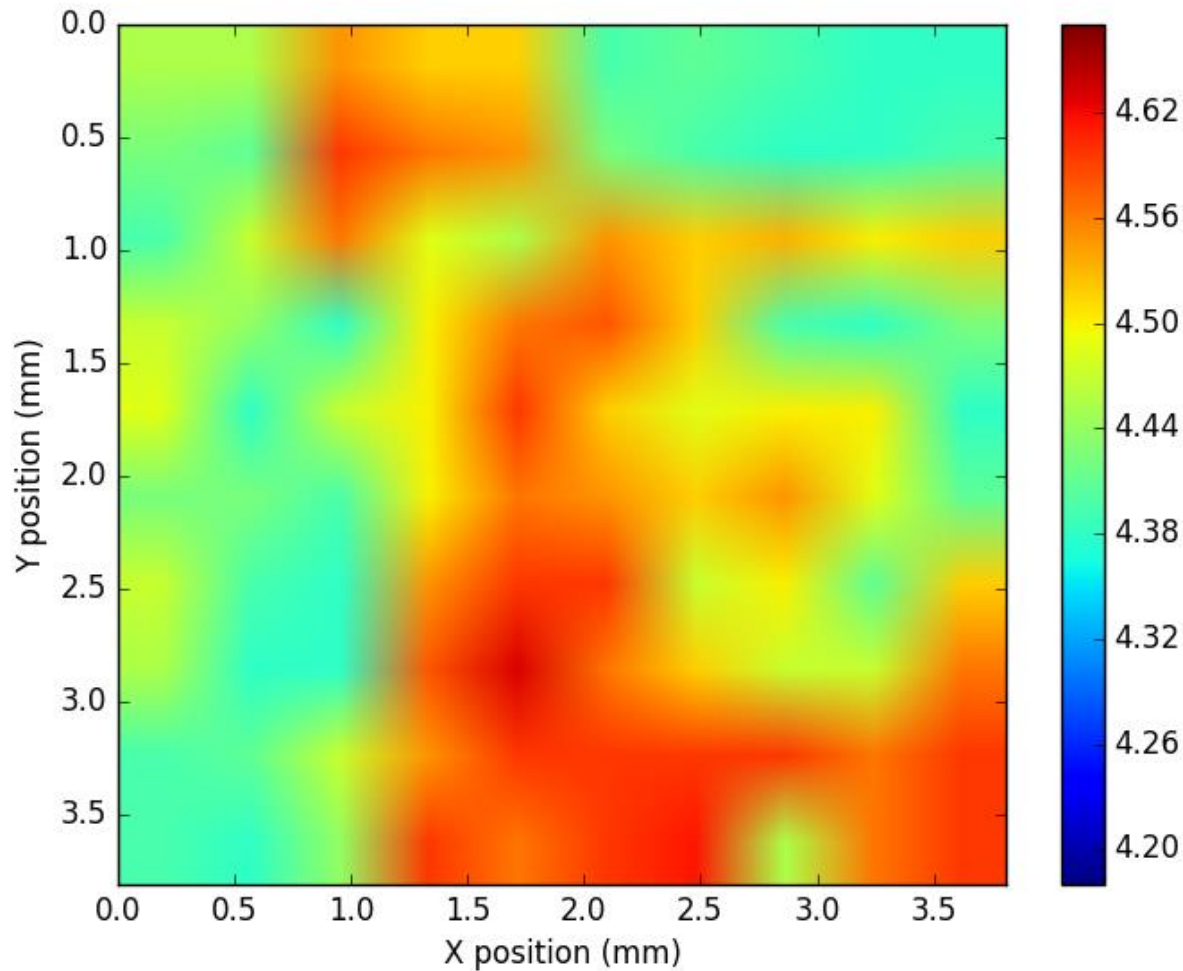
All spectra



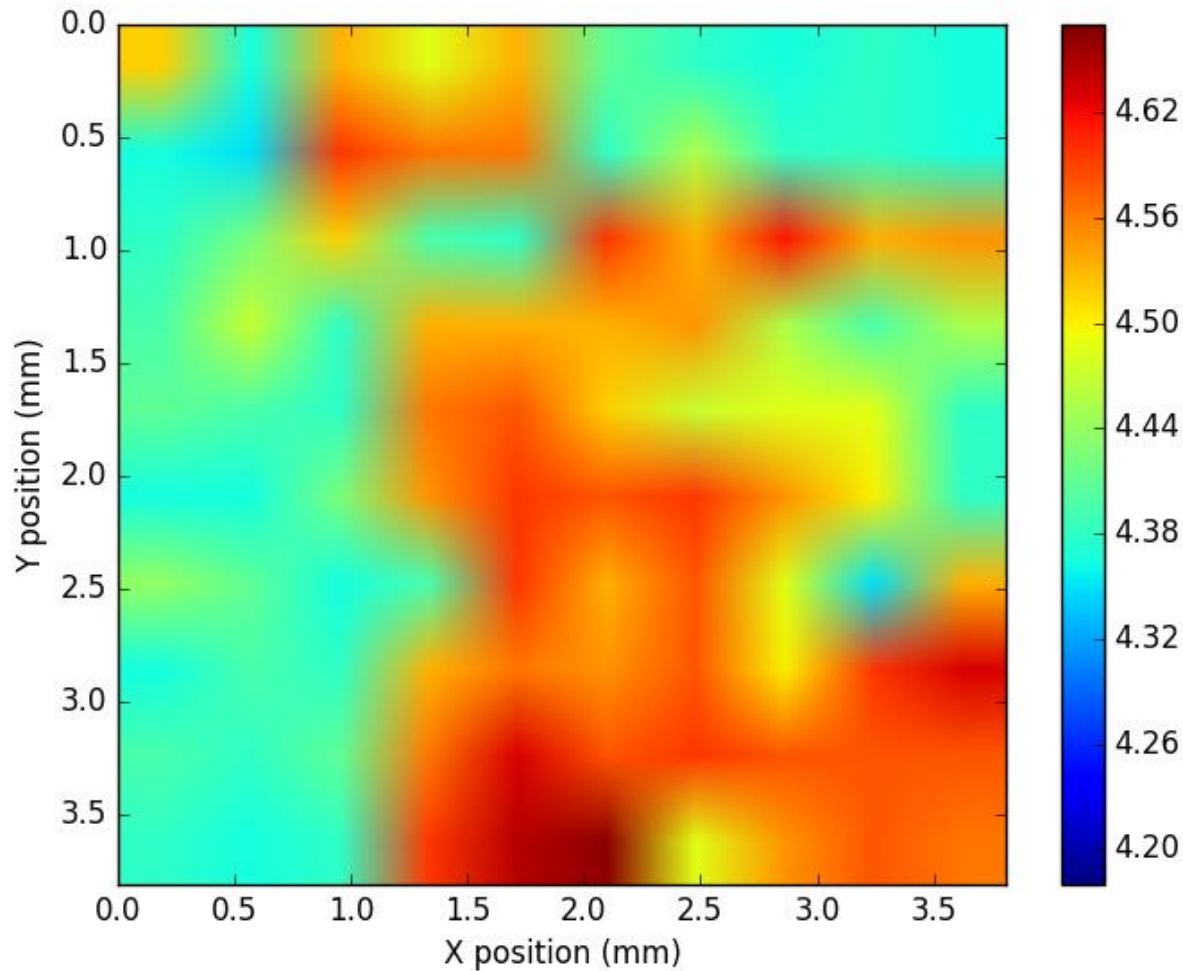
Each spectra:

- Y from 29 K (top) to 38 K (bottom)
- X from ~ 300 meV (left, $3.92 \mu\text{m}$) to 250 meV (right, $4.97 \mu\text{m}$)

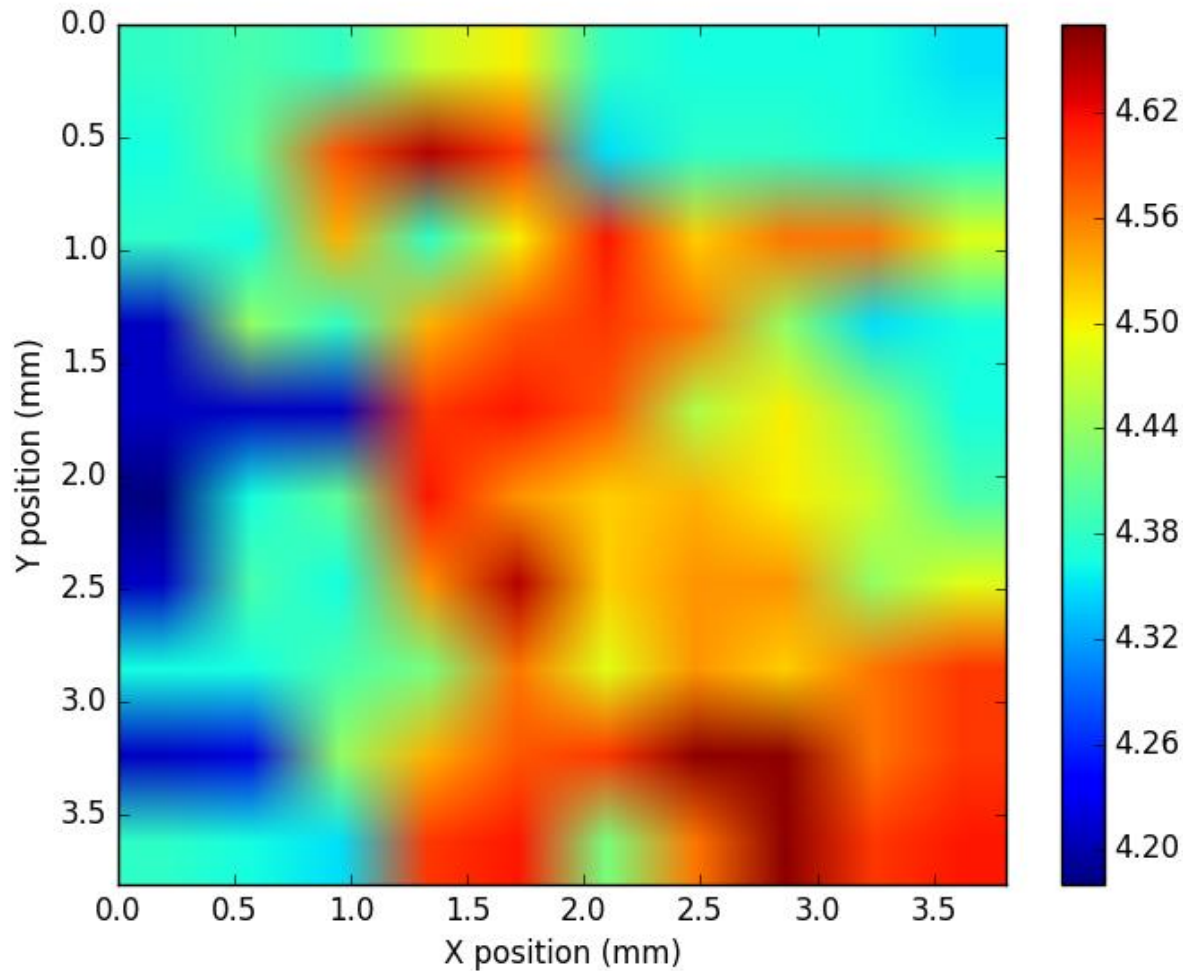
Peak wavelength in μm (29 K)



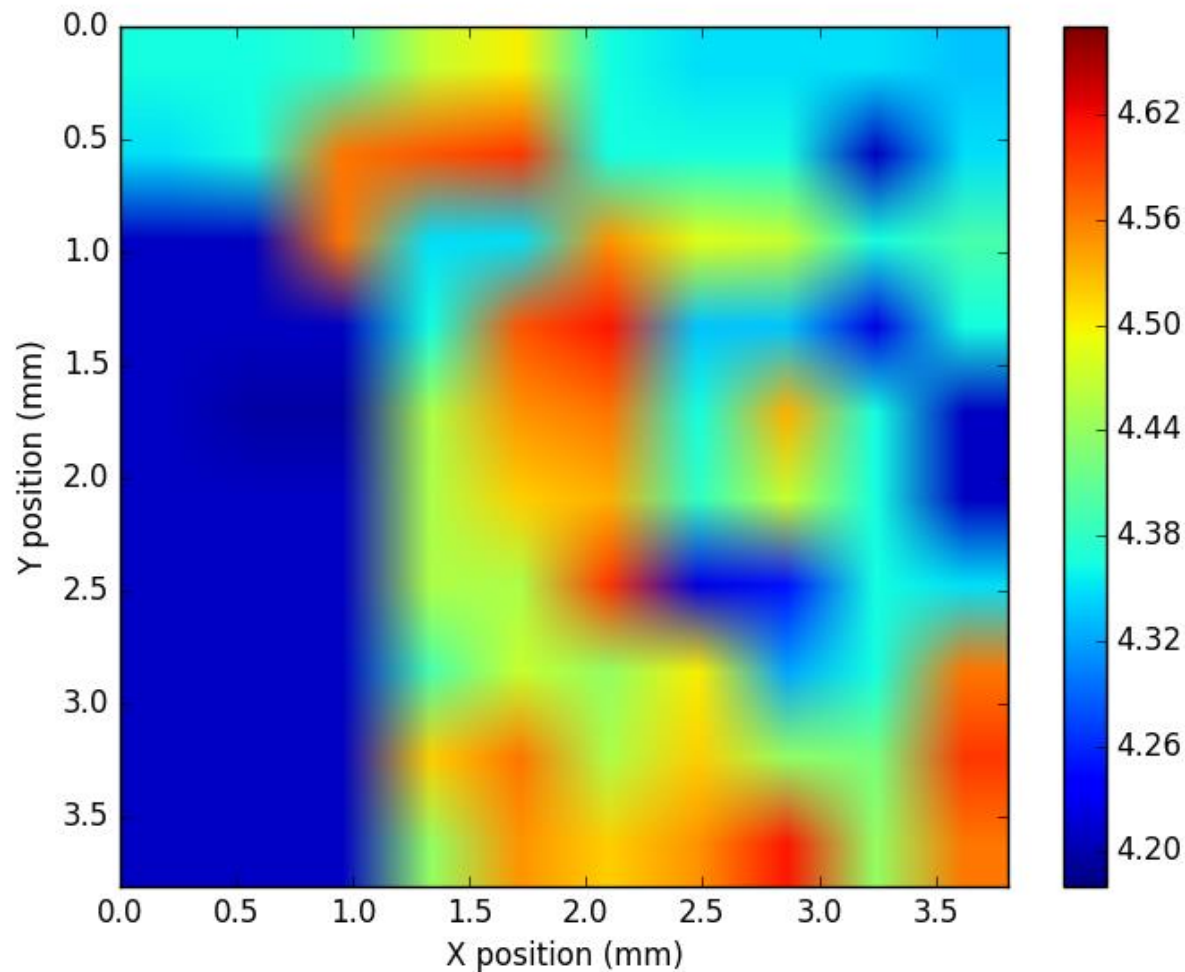
Peak wavelength in μm (30 K)



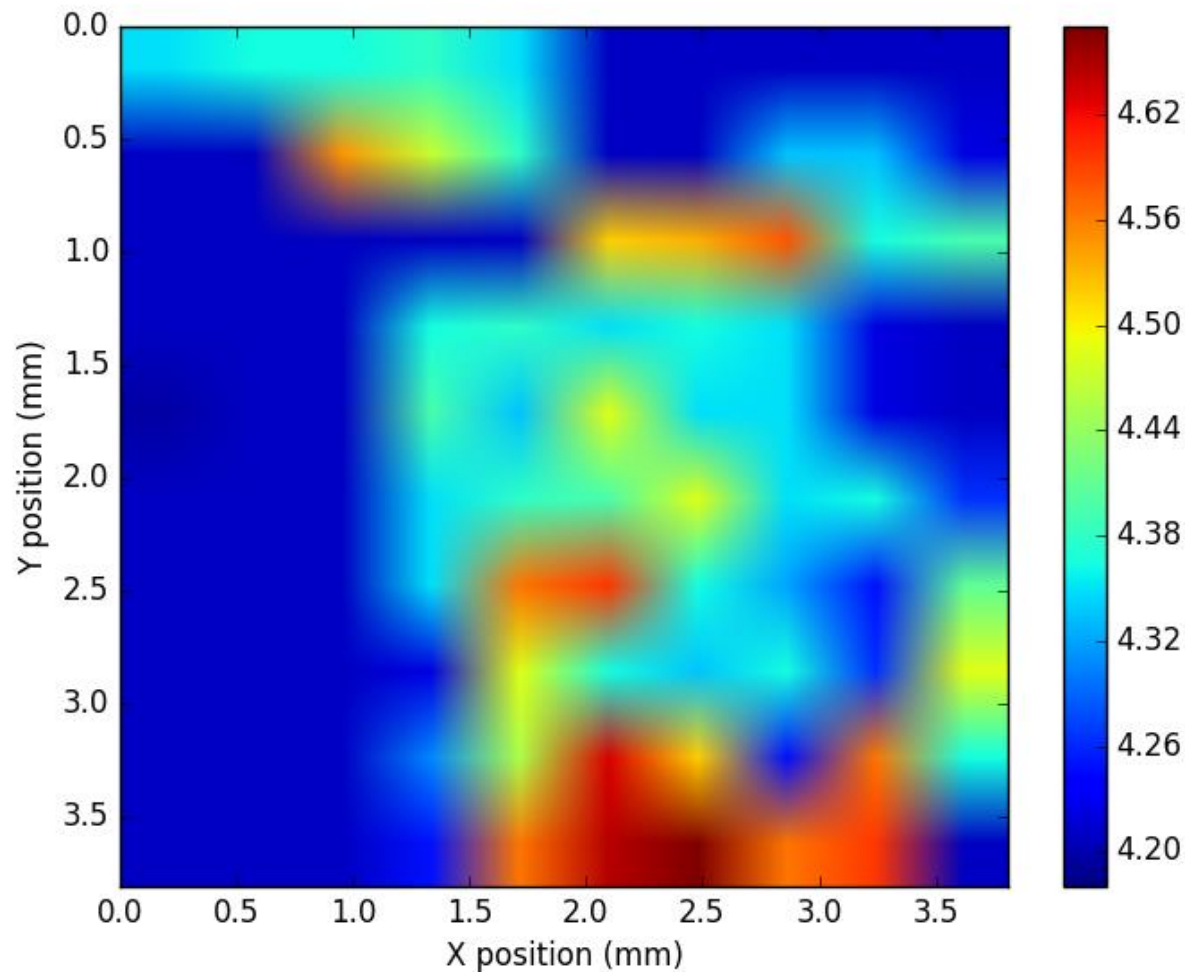
Peak wavelength in μm (31 K)



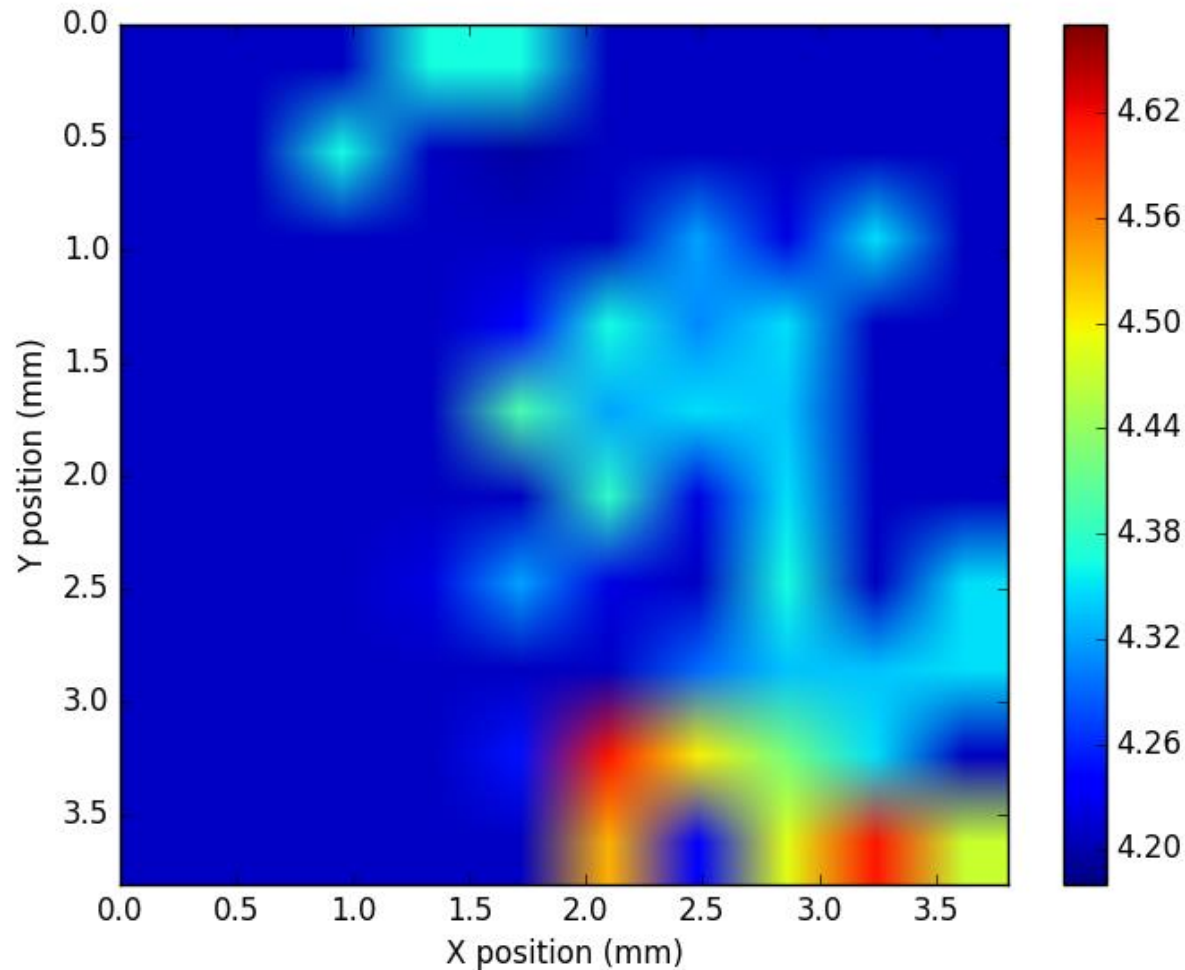
Peak wavelength in μm (32 K)



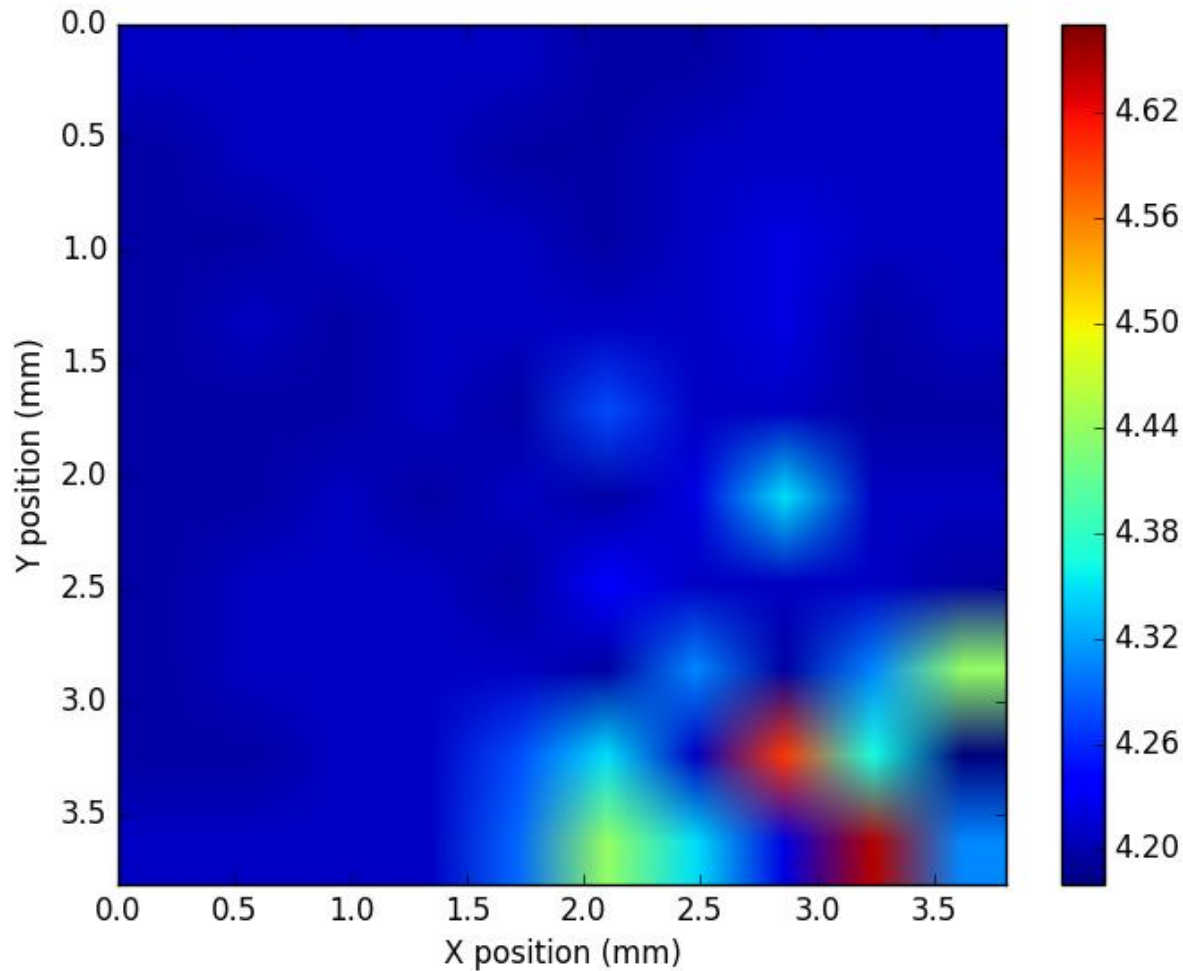
Peak wavelength in μm (33 K)



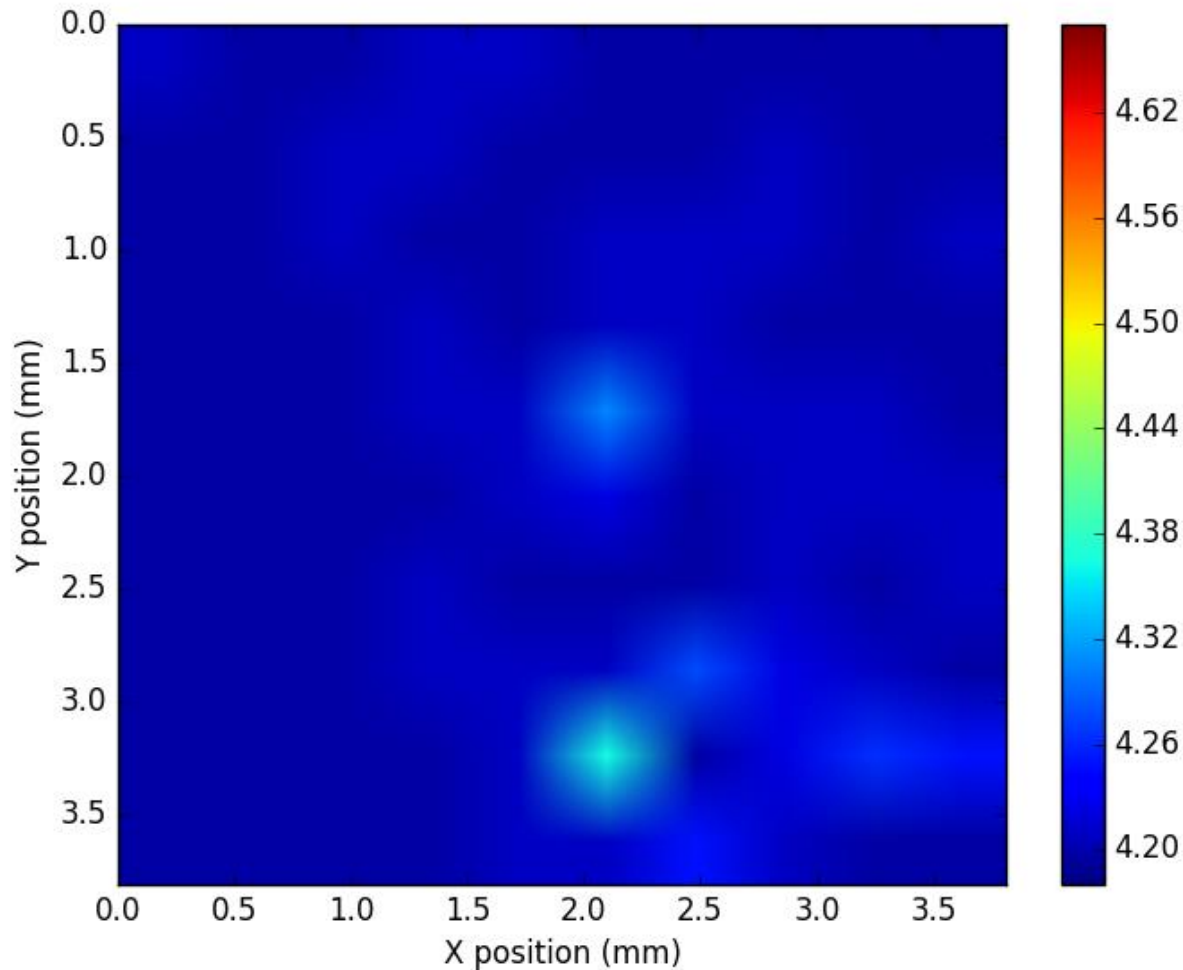
Peak wavelength in μm (34 K)



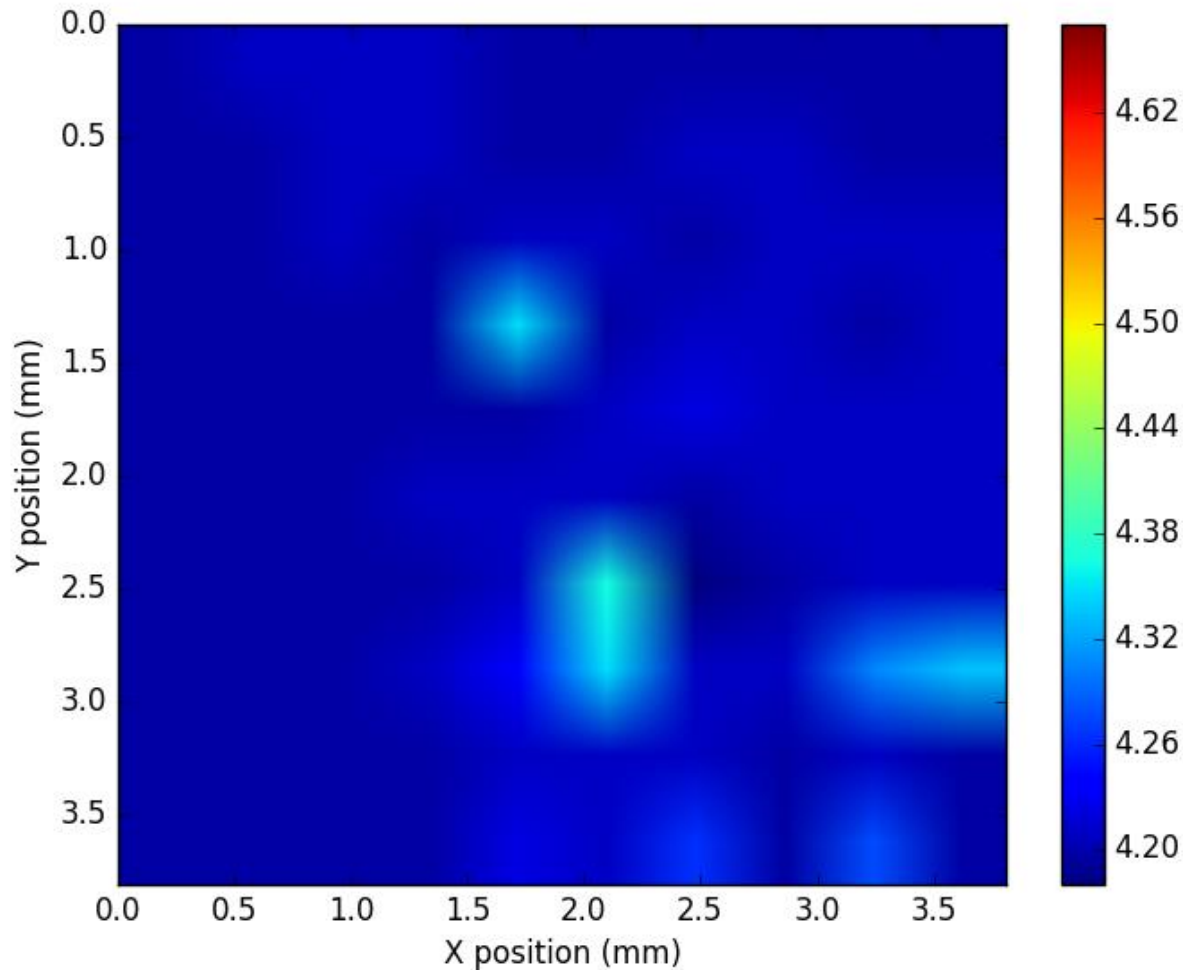
Peak wavelength in μm (35 K)



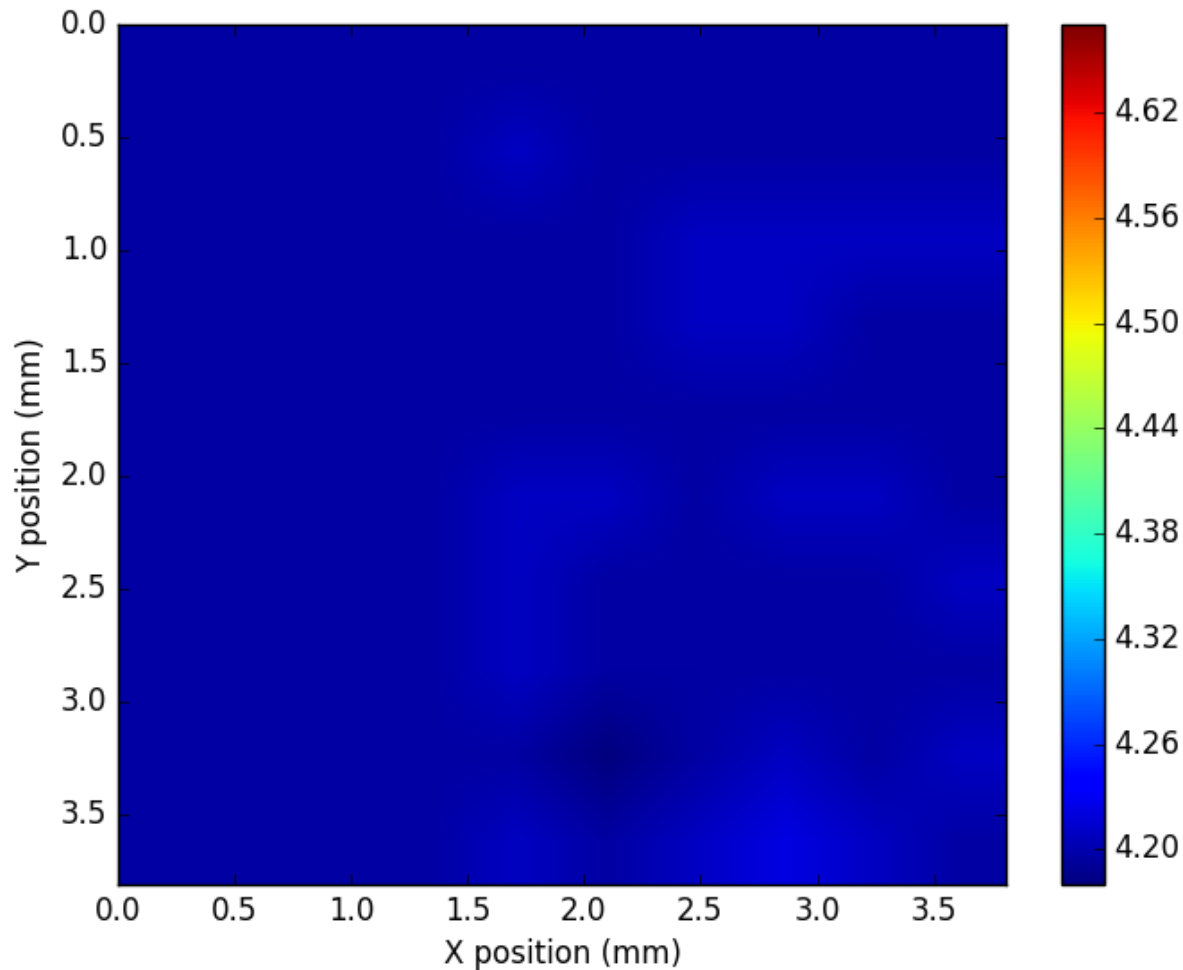
Peak wavelength in μm (36 K)



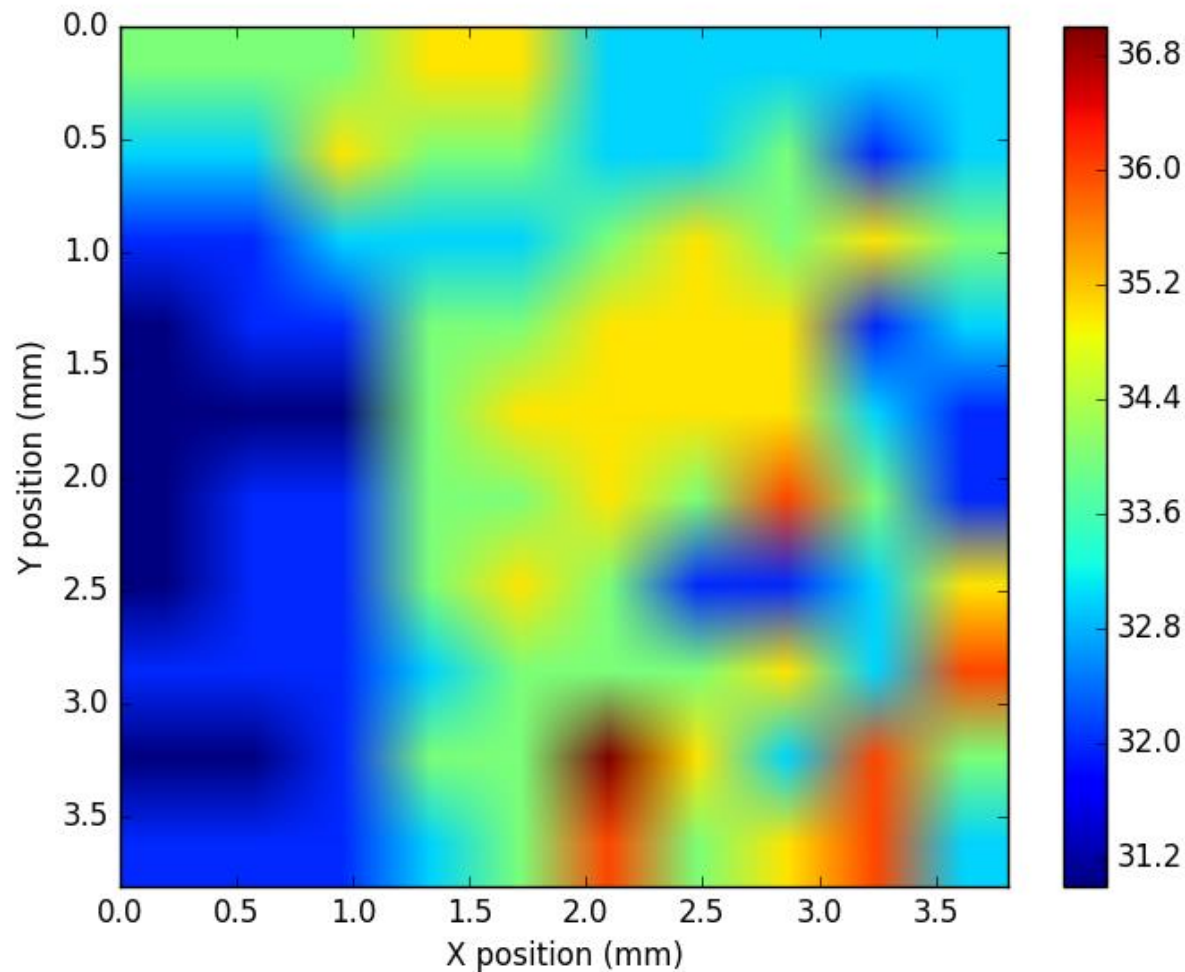
Peak wavelength in μm (37 K)



Peak wavelength in μm (38 K)

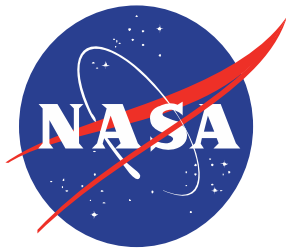


Temperature (K) of transition to “extended state”



Conclusions

- InAsSb/InSb digital alloy shows 14 meV blue shift in photoluminescence peak at 35 K...
 - ...due to appearance of second peak!
- Below this transition minority carrier lifetime increases from ~500-600 ns to ~1800 ns
- Consistent with “localized states” hypothesis
- Effect varies with spatial position at mm scale
- Variability includes transition temp., intensity, num/shape of peaks
- Variability qualitatively different from “temperature gradient” or “edge effect” null hypothesis
- This effect is consistent with monolayer and “sub-monolayer” fluctuations in the layer thicknesses



Jet Propulsion Laboratory
California Institute of Technology